

The induction of two biosynthetic enzymes helps *Escherichia coli* sustain heme synthesis and activate catalase during hydrogen peroxide stress

Stefano Mancini[†] and James A. Imlay*

Department of Microbiology, University of Illinois,
Urbana, IL 61801, USA.

Summary

Hydrogen peroxide pervades many natural environments, including the phagosomes that mediate cell-based immunity. Transcriptomic analysis showed that during protracted low-grade H₂O₂ stress, *Escherichia coli* responds by activating both the OxyR defensive regulon and the Fur iron-starvation response. OxyR induced synthesis of two members of the nine-step heme biosynthetic pathway: ferrochelatase (HemH) and an isozyme of coproporphyrinogen III oxidase (HemF). Mutations that blocked either adaptation caused the accumulation of porphyrin intermediates, inadequate activation of heme enzymes, low catalase activity, defective clearance of H₂O₂ and a failure to grow. Genetic analysis indicated that HemH induction is needed to compensate for iron sequestration by the mini-ferritin Dps. Dps activity protects DNA and proteins by limiting Fenton chemistry, but it interferes with the ability of HemH to acquire the iron that it needs to complete heme synthesis. HemF is a manganoprotein that displaces HemN, an iron–sulfur enzyme whose synthesis and/or stability is apparently problematic during H₂O₂ stress. Thus, the primary responses to H₂O₂, including the sequestration of iron, require compensatory adjustments in the mechanisms of iron-cofactor synthesis. The results support the growing evidence that oxidative stress is primarily an iron pathology.

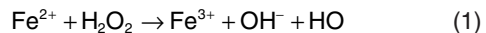
Introduction

Life evolved in an anoxic world and now must find ways to persist in an oxic one. One of the key oxidative threats to oxygen-tolerant organisms is hydrogen peroxide (H₂O₂).

Accepted 8 February, 2015. *For correspondence. E-mail jimlay@illinois.edu; Tel. (217)-333-5812; Fax 217-244-6697. †Present address: Department of Fundamental Microbiology, University of Lausanne, 1015 Lausanne, Switzerland.

This species is constantly formed within aerobic cells via the adventitious oxidation of redox enzymes (Massey *et al.*, 1969; Seaver and Imlay, 2001b; Imlay, 2013). Virtually all organisms employ catalases and peroxidases to keep the steady-state level of endogenous H₂O₂ below the threshold of toxicity. However, H₂O₂ is also formed in extracellular environments through the chemical oxidation of reduced thiols or metals, through photochemistry, through the redox-cycling of antibiotic molecules, through the release of H₂O₂ by lactic-acid bacteria and most prominently through the deliberate actions of the NADPH oxidases of amoebae, plants and mammalian phagocytes (Glass *et al.*, 1986; Mehdy, 1994; Bedard *et al.*, 2007). Hydrogen peroxide is small and uncharged, so it readily crosses cell membranes (Seaver and Imlay, 2001b). Once inside the cell, H₂O₂ exerts both static and lethal effects. The key goals of the field are to identify the injuries that H₂O₂ creates and to reveal the strategies that cells use to avoid or mitigate them.

Studies of H₂O₂ lethality in the model organism *Escherichia coli* determined that cell death was due to DNA damage, which arose via the Fenton reaction (Imlay *et al.*, 1988):



The cell maintains a pool of unincorporated iron that is used to metallate nascent iron proteins (Srinivasan *et al.*, 2000). This loose iron sticks to the surfaces of biomolecules, including nucleic acids, and the DNA damage arises when hydroxyl radicals made at that site react with the DNA (Rai *et al.*, 2001).

Those studies were conducted by adding millimolar concentrations of H₂O₂ to relatively dense cultures of bacteria, and their relevance could be questioned because such high concentrations are unlikely in natural habitats. Some clarity was reached through the investigation of the OxyR response, an inducible defense system that was first studied in enteric bacteria. OxyR is a transcription factor that is activated when H₂O₂ oxidizes its sensory cysteine residue, triggering the formation of a disulfide bond that locks the protein into an activated conformation (Lee *et al.*, 2004). In this form, it stimulates the transcription of a set of operons that are scattered around the chromosome.

Careful study revealed that as little as 0.1–0.2 µM, intracellular H₂O₂ is sufficient to activate the OxyR response (Aslund *et al.*, 1999). Because scavenging enzymes reduce the intracellular H₂O₂ concentration below that of the extracellular environment, it appears that ~ 0.5 µM extracellular H₂O₂ is an activating dose (Seaver and Imlay, 2001b). Implicitly, this represents a concentration that *E. coli* recognizes as a hazard.

Proteomics and, later, microarray experiments have identified members of the OxyR regulon (Morgan *et al.*, 1986; Zheng *et al.*, 2001). These include AhpCF, originally identified as an alkylhydroperoxide reductase and now recognized as an NADH peroxidase that scavenges the endogenous H₂O₂ (Jacobson *et al.*, 1989; Seaver and Imlay, 2001a; Parsonage *et al.*, 2008). Catalase G (also known as HPI) is an inducible enzyme that is especially effective at the higher doses of H₂O₂ that saturate the Ahp system (Seaver and Imlay, 2001a). Dps is a ferritin-like protein that sequesters intracellular unincorporated iron, thereby greatly diminishing the amount of Fenton chemistry that damages DNA and proteins (Ilari *et al.*, 2002; Park *et al.*, 2005; Anjem and Imlay, 2012). The Suf proteins form a complex that provides iron–sulfur clusters to apoenzymes; it replaces the housekeeping Isc system, which is inactivated during H₂O₂ stress (Jang and Imlay, 2010; Py and Barrias, 2010). The [4Fe–4S] clusters of dehydratases are primary targets of H₂O₂, and the continuous repair of these clusters by Suf helps to avert the failure of the TCA cycle and branched-chain biosynthetic pathways, which contain such enzymes (Jang and Imlay, 2007). Finally, the induction of the MntH manganese importer protects non-redox mononuclear enzymes from H₂O₂ (Kehres *et al.*, 2002; Sobota and Imlay, 2011; Anjem and Imlay, 2012; Sobota *et al.*, 2014). The mononuclear enzymes normally employ ferrous iron as a cofactor, but during H₂O₂ stress, the apparent replacement of that metal by manganese allows activity to be sustained without the threat of Fenton chemistry in the active site. Interestingly, homologs of many OxyR-regulon members are induced by H₂O₂ in bacteria that use PerR as an alternative sensor protein (Helmann *et al.*, 2003; Lee and Helmann, 2006).

To test the impact of H₂O₂ stress upon cell physiology, it would be ideal to expose cells for extended periods of time to concentrations of H₂O₂ that might be encountered in nature. Using the activation point of OxyR as a guide, one estimates that this logic recommends H₂O₂ exposures that cause cytoplasmic H₂O₂ to moderately exceed 0.2 µM. Unfortunately, when low-micromolar doses of H₂O₂ are added to standard cultures as a single bolus, the cells degrade the H₂O₂ far too quickly for growth defects to be detected. In contrast, in nature most H₂O₂ formation is continuous and bacterial densities are typically low, so H₂O₂ levels are stable and stress is protracted. To achieve a similar situation in the laboratory, workers have resorted

to using redox-cycling antibiotics, which complicate the situation by producing superoxide, or to using catalase- and peroxidase-deficient mutants that do not degrade H₂O₂. When such mutants of *E. coli*[Δ katG Δ katE Δ ahpCF], denoted Hpx[−] (Seaver and Imlay, 2001a) are cultured in aerobic media, endogenous autoxidation reactions produce H₂O₂ that immediately equilibrates across the cell membrane, establishing an intracellular concentration of ~ 0.5–1 µM (Seaver and Imlay, 2001b). This felicitous dose has proved useful in identifying targets of injury and in demonstrating the roles of OxyR-induced proteins.

In this study, we have employed Hpx[−] mutants to determine the full transcriptome of *E. coli* during chronic H₂O₂ stress. The data replicate the induction of known members of the OxyR regulon. In addition, they demonstrate that the combination of iron oxidation and rerouting into Dps leaves the cell iron deficient. This is problematic for heme synthesis, which under the circumstance is critical for the induction of catalase. The OxyR response resolves the dilemma by elevating the titer of ferrochelatase and by replacing the iron–sulfur-dependent HemN protein with an iron-independent isozyme. In aggregate, the data demonstrate that physiological doses of H₂O₂ comprise an iron-centric stress.

Results

The transcriptome of H₂O₂-stressed cells

Zheng and Storz performed a microarray analysis of *E. coli* during exposure to 1 mM H₂O₂, and their study identified an array of genes that respond to the OxyR transcription factor (Zheng *et al.*, 2001). We wished to complement that approach by sequencing the transcripts of cells that grew for an extended period in the presence of much lower, physiological levels of H₂O₂. This strategy might reveal shifts in the transcriptome that are driven not only by OxyR itself but also by the impact that oxidative stress has upon cell metabolism.

To impose chronic oxidative stress, we used Hpx[−] strains, which lack the primary H₂O₂-scavenging activities. Because H₂O₂ is constantly formed inside cells by the autoxidation of redox enzymes, aerated Hpx[−] mutants accumulate ~ 1 µM intracellular H₂O₂. The OxyR transcription factor is activated when levels of H₂O₂ exceed ~ 0.2 µM, and so Hpx[−] strains fully express the OxyR regulon. In normal H₂O₂-stressed cells, the OxyR-driven induction of the KatG catalase imposes a requirement for substantial heme synthesis, and this demand might have its own consequences. To test this possibility, we used a katG allele in which the deletion of a polypeptide loop eliminates catalase activity and yet preserves the ability of the protein to bind heme (Li and Goodwin, 2004). In addition, the heme status of this enzyme can be tracked

because the presence of the heme allows the protein to exhibit dye-peroxidase activity in cell extracts. Thus, in this strain, which we denote as Hpx²⁻, chronic H₂O₂ stress occurs (Fig. S1). This situation mimics the experience of bacteria in natural habitats that contain constant sources of exogenous H₂O₂.

Prior studies indicated that H₂O₂ stress disrupts biosynthetic pathways and iron homeostasis (Jang and Imlay, 2007; 2010; Varghese *et al.*, 2007; Sobota *et al.*, 2014). These effects are obscured when cells are grown in classic Lysogeny broth (LB), an extremely rich medium that provides ample nutrients and high levels of iron. Therefore, the Hpx²⁻ strain was instead grown in a minimal glucose medium. The only other biomolecules that were supplied were Phe, Trp and Tyr, as even low levels of H₂O₂ block their biosynthetic pathway (Sobota *et al.*, 2014). Cells were systematically maintained in early exponential phase for at least 10 generations prior to RNA harvest (Experimental procedures) so that their physiology had fully adapted to H₂O₂-stress conditions. The doubling times under these conditions were 49 ± 1 min for three parallel cultures of wild-type cells and 138 ± 7 min for three Hpx²⁻ cultures (Fig. S2).

Table S6 represents the transcriptome of the Hpx²⁻ mutant compared with that of unstressed wild-type cells. Several patterns are immediately clear. Virtually all of the most strongly induced genes belong to the OxyR, SOS or Fur regulons (Table S1). Derepression of the OxyR regulon was no surprise, and all genes known to be within it were substantially induced (Table S2). Activation of the SOS response indicated that at least some of the cells struggled to replicate their DNA, presumably due to oxidative lesions arising from Fenton chemistry (Goerlich *et al.*, 1989; Asad *et al.*, 1997; Park *et al.*, 2005). Expression of the Fur regulon indicated that the Fur repressor lacked its ferrous cofactor. This effect could derive from several factors. H₂O₂ directly oxidizes the solvent-exposed iron atoms of mononuclear proteins, causing the iron to dissociate (Anjem and Imlay, 2012), and such an effect would directly deactivate Fur protein (Varghese *et al.*, 2007). The chemical oxidation of ferrous iron by H₂O₂ might additionally lead to ferric deposition upon molecular surfaces, diminishing ferrous iron availability. Finally, Dps, a ferritin-like protein that was strongly induced by OxyR, depletes the cellular pool of ferrous iron by sequestering it (Altuvia *et al.*, 1994; Ilari *et al.*, 2002; Park *et al.*, 2005).

The shrinking of cellular iron pools constitutes a problem for the assembly of iron-containing cofactors. Enzymic iron–sulfur clusters are initially built upon a scaffold protein by the Isc machinery (Roche *et al.*, 2013). This system fails during iron starvation or H₂O₂ stress, and in both circumstances the cell responds by inducing the *suf* operon (Kehres *et al.*, 2002; Nachin *et al.*, 2003; Jang and Imlay, 2010). The Suf system comprises a secondary

iron–sulfur assembly system that is particularly adept at building clusters when iron levels are low (Outten *et al.*, 2004). Iron is also incorporated into heme, and so we were interested to know whether heme synthesis might be problematic during H₂O₂ exposure. If so, it seemed likely that analogous adaptations might be incorporated into the stress response, particularly because the induction of catalase elevates heme demand. This issue is the focus of this report.

hemH is induced by OxyR during H₂O₂ stress

The synthesis of heme entails nine reactions that convert glutamyl-tRNA to protoporphyrin IX. Ferrochelatase, encoded by *hemH*, then completes the process by inserting a ferrous iron atom (Fig. 1A). Microarray experiments by Zheng and Storz identified *hemH* as a member of the *E. coli* OxyR regulon; no other *hem* genes were implicated (Zheng *et al.*, 2001). Their data indicated that *hemH* was induced 11-fold when cells were exposed to a bolus of 1 mM H₂O₂. DNase I footprinting indicated that the regulation by OxyR was likely to be direct (Zheng *et al.*, 2001). Our transcriptome data indicated that *hemH* was induced 14-fold in the Hpx²⁻ strain. We also observed that the *hemF* gene was induced sixfold, whereas the eight other *hem* genes remained at basal levels (Fig. 1B).

Our investigation focused first upon the rationale for *hemH*/induction. In the Hpx²⁻ strain, *katG* transcription was induced 60-fold. Because rapid catalase synthesis would elevate heme demand, we took a further look to see whether part or most of the OxyR-dependent induction of *hemH* might be mediated by a yet-unidentified transcription factor that senses a drop in the heme pool. To do so, we used quantitative real-time polymerase chain reaction (qPCR) to compare the degree of *hemH* induction in the Hpx²⁻ strain, which synthesizes the heme-binding (but inactive) catalase protein, with that of an Hpx⁻ strain in which the *katG* gene has been fully deleted. We found that the degree of induction was equivalent in the two strains (Fig. 2A). The same result was obtained using *hemH'-lacZ*⁺ fusions (Fig. 2B). Induction was equally rapid (Fig. S3). Moreover, quantitatively similar induction occurred when unstressed wild-type cells were transformed with the *oxyR2* plasmid, which encodes a constitutively active form of OxyR (Fig. 2A). We conclude that during H₂O₂ stress OxyR specifically induces *hemH*, which fits the footprinting data of Zheng and Storz. Furthermore, there is no apparent transcriptional feedback to *hemH* arising from the elevated heme demand itself.

HemA levels are not elevated during H₂O₂ stress

We sought to verify that *hemH* and *hemF* were distinct among the *hem* genes in being induced during H₂O₂ stress.

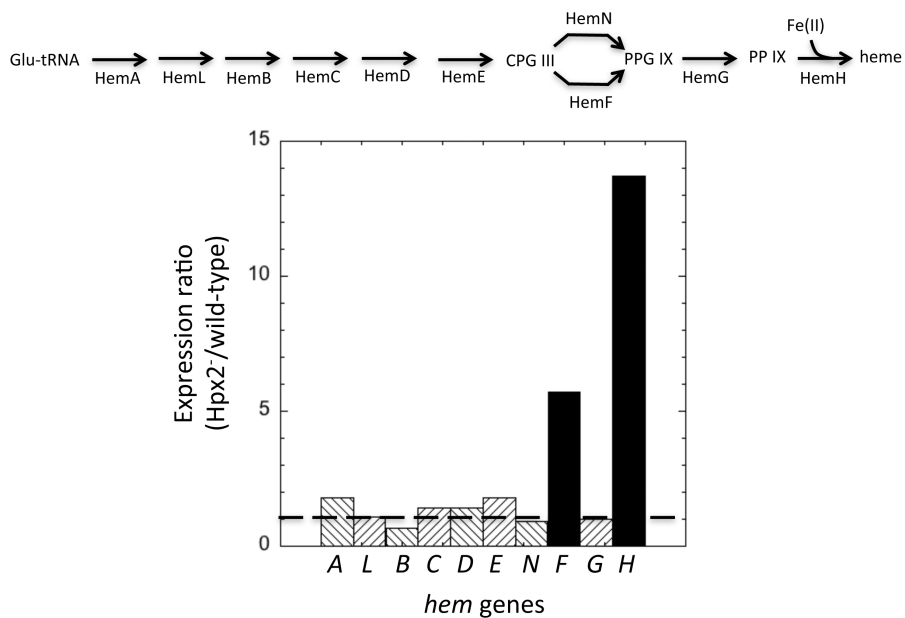


Fig. 1. Heme biosynthetic pathway of *Escherichia coli* K-12. (Top) CPG III is coproporphyrinogen III; PP IX is protoporphyrin IX. HemN and HemF are coproporphyrinogen III oxidases, and HemH is ferrochelatase. (Bottom) Expression of heme biosynthetic genes in H_2O_2 -stressed $\text{Hpx}2^-$ mutants (SMA1385) compared with wild-type cells (MG1655), as indicated by RNA-sequencing analysis.

HemA (glutamyl-tRNA reductase) catalyzes the first dedicated step in heme synthesis (Fig. 1), and prior studies suggested that under standard conditions, this reaction is rate-limiting for pathway flux (Woodard and Dailey, 1995; Jones and Elliott, 2010). If the basal levels of heme synthetic enzymes were inadequate for full catalase induction,

one might expect HemA levels to rise during H_2O_2 stress. Therefore, this gene was the most likely target for any transcriptional control. Although the published microarray studies had not identified *hemA* (or any *hem* gene other than *hemH*) as responsive to H_2O_2 exposure (Zheng *et al.*, 2001; Lee *et al.*, 2009; Dwyer *et al.*, 2014), this result was

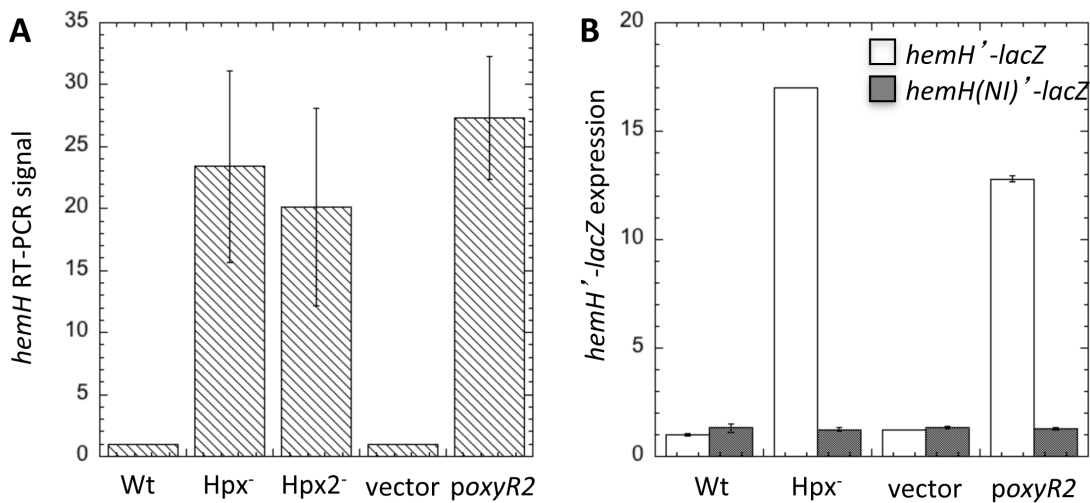


Fig. 2. The *hemH* gene is induced during H_2O_2 stress by OxyR.

A. qPCR quantification of *hemH* transcripts in strains growing exponentially in oxic glucose medium. Strains used were MG1655 (WT), LC106 (Hpx^-), SMA1383 ($\text{Hpx}2^-$), SMA1151 (WT with vector) and SMA1149 (WT with *poxyR2* plasmid). Data represent the mean of three independent experiments.

B. Expression of *hemH*:*lacZ* and *hemH(NI)*:*lacZ* transcriptional fusions in aerobic LB medium. Data represent the mean of three independent experiments. The *hemH*:*lacZ* strains were SMA1023 (WT), SMA1119 (Hpx^-), SMA1061 (WT with vector), SMA1025 (WT with *poxyR2* plasmid). The *hemH(NI)*:*lacZ* strains were SMA1049 (WT), SMA1079 (Hpx^-), SMA1063 (WT with vector) and SMA1055 (WT with *poxyR2* plasmid).

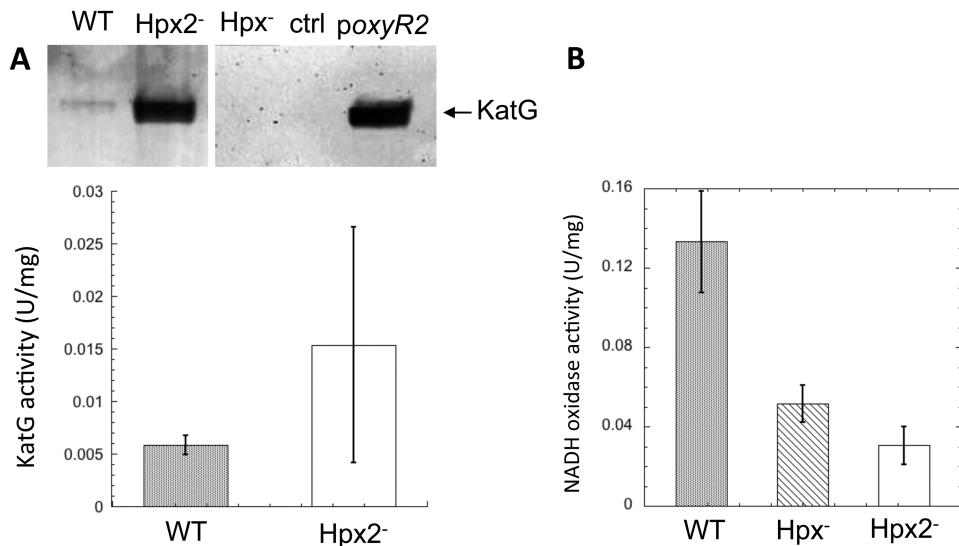


Fig. 3. The heme proteins KatG and cytochrome oxidases are poorly activated during H_2O_2 stress.

A. Top: The KatG protein content is ~14-fold higher in Hpx²⁻ cells than WT cells. Cells were grown in oxic glucose medium, and KatG protein content was quantified by western blotting and densitometry. Lanes contained equivalent total protein. Bottom: Hpx²⁻ strains exhibited only 2.5-fold higher KatG peroxidase activity than WT cells. Both strains harbored the *katGΔFG* allele, which produces a KatG protein with heme-dependent peroxidase activity.

B. The NADH oxidase activity of the respiratory chain is diminished in Hpx⁻ and Hpx²⁻ strains. NADH dehydrogenase activities were equivalent (Fig. S5), indicating that the disparities in NADH oxidase activities result reflect differences in cytochrome oxidase activities. All data represent three independent experiments. Strains used in these experiments were SMA1379 (*katGΔFG*), LC106 (Hpx⁻) and SMA1383 (Hpx²⁻).

not definitive: the millimolar H_2O_2 doses that were used in those experiments were sufficient to block protein synthesis and thus would not have triggered any increase in heme demand. In contrast, the Hpx²⁻ RNA sequencing data were obtained under conditions in which catalase synthesis had been induced for an extended time; those data showed a very minor increase in *hemA* transcription (Fig. 1). This result was double-checked with a *hemA'-lacZ* construct. Fusion expression was only slightly higher (~1.7 times) in the Hpx²⁻ cells than in noninduced wild-type cells (Fig. S4). Moreover, an equivalent effect was observed in the catalase-null Hpx⁻ cells, indicating that the minimal transcriptional activation was not attributable to an increase in heme demand. The introduction of the *poxyR2* plasmid into wild-type cells caused the strong induction of catalase synthesis but did not trigger significant *hemA* expression. Thus, neither OxyR activation per se nor rapid catalase synthesis boosts *hemA* transcription.

Recent work has suggested that HemA levels can respond to heme sufficiency at the level of protein lifetime: when intracellular heme levels are adequate, HemA binds heme and becomes vulnerable to rapid degradation by the Lon and ClpAP proteases (Wang *et al.*, 1997; 1999; Jones and Elliott, 2010). Conversely, heme scarcity triggers stabilization of heme-free HemA protein. In principle, during H_2O_2 stress HemA quantities might keep pace with heme demand via this post-transcriptional mechanism. However, western blot analysis demonstrated that HemA protein

levels were no different in Hpx²⁻ strains with high catalase synthesis than in wild-type cells where catalase synthesis was far lower (Fig. S4). These results imply that even during H_2O_2 -mediated induction of catalase synthesis, most enzymes in the pathway – including the usual rate-determining one – are fully adequate. The implication, then, is that H_2O_2 stress somehow creates a situation in which the ferrochelatase step becomes a specific bottleneck, and *hemH* induction by OxyR may be a way to solve that problem.

H_2O_2 -stressed cells are inefficient at providing heme to enzymes

If heme synthesis is difficult during H_2O_2 stress, the activation of heme proteins may lag behind their synthesis. Indeed, enzyme assays of heme-dependent enzymes revealed activity defects. After 3 h of aeration, the KatG protein titers in the Hpx²⁻ strain were 14-fold higher than in the unstressed wild-type strain, consistent with the transcriptional induction of *katG* by H_2O_2 -activated OxyR (Fig. 3A). However, the KatG-dependent peroxidase activity was elevated only 2.6-fold, suggesting that much of the enzyme lacked heme. The other prominent heme-requiring proteins in aerobic cells are the cytochrome bo and bd oxidases that terminate the respiratory chain (Table S3). Inverted membrane vesicles were prepared, and NADH oxidase activity was assayed. Activity in the Hpx⁻ strain

was only 40% that of wild-type cells. In the *Hpx2⁻* strain, which induces heme-containing KatG, the level was further reduced to 23% (Fig. 3B). This NADH oxidase activity depends upon the activities of both NADH dehydrogenase and cytochrome oxidase; specific assays showed near-normal levels of NADH dehydrogenase activity, indicating that the oxidase failure represented low cytochrome oxidase function (Fig. S5). The transcriptome analysis showed that both enzyme complexes were transcribed at normal rates, so that the lack of the heme cofactor was the probable culprit for the reduced oxidase activity. The enzyme defect is even larger than these numbers suggest, as in wild-type membranes the NADH dehydrogenase constitutes the rate-limiting step; thus, some decline in cytochrome oxidase activity occurs before overall oxidase flux is diminished. This decline could potentially exacerbate problems with heme synthesis, as the protoporphyrinogen IX oxidase HemG delivers electrons into the respiratory chain (Mobius *et al.*, 2010). In sum, these data indicate that heme provision to heme-requiring proteins is less efficient during H₂O₂ stress than in unstressed cells, and this inadequacy is exacerbated by the induction of heme-requiring catalase.

The induction of *hemH* is necessary for adequate heme synthesis during H₂O₂ stress

The fact that the OxyR regulon specifically controls *hemH* suggested that the ferrochelatase step potentially comprises a specific biosynthetic bottleneck during H₂O₂ stress. To probe the importance of *hemH* induction, we deleted the OxyR binding cassette upstream of *hemH*, resulting in a strain in which *hemH* is noninducible [denoted *hemH(NI)*]. A *hemH(NI)-lacZ*⁺ fusion was constructed to confirm the effect of this mutation upon transcriptional levels. Loss of the OxyR site did not diminish basal expression of this fusion, but during H₂O₂ stress induction no longer occurred (Fig. 2B).

The mutation had only modest effects upon the growth behavior of *Hpx⁻* strains, with no effect at all in iron-rich LB medium and only a modest slowing in low-iron minimal medium (data not shown). However, the combined intracellular levels of protoporphyrinogen IX and protoporphyrin IX, the ferrochelatase substrate, increased fivefold above normal levels in H₂O₂-stressed *Hpx2⁻* cells, and they increased 18-fold when *hemH* was noninducible (Fig. 4).

The significance of *hemH* induction was examined in otherwise wild-type cells under conditions in which successful heme synthesis would provide a growth advantage. When confronted with a bolus of exogenous H₂O₂ (0.5 mM), the wild-type (*hemH⁺*) cells resumed growth after a lag period, but the *hemH(NI)* cells did not (Fig. 5A). The source of the defect is that the wild-type cells were able to induce high titers of catalase activity during the lag period,

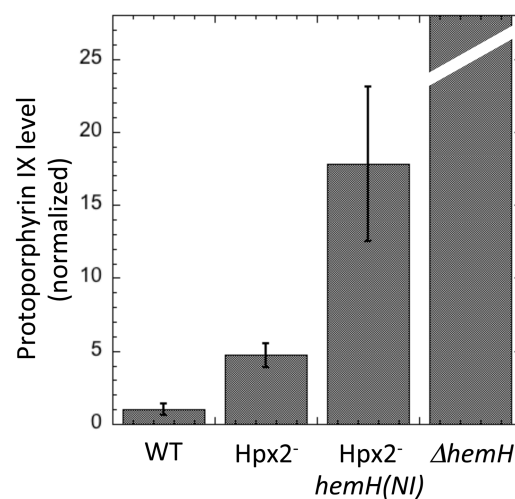


Fig. 4. Protoporphyrinogen/protoporphyrin IX accumulate in H₂O₂-stressed cells, especially when *hemH* induction is blocked. Cells were grown in aerobic glucose medium, and the protoporphyrin IX content of cell extracts was measured by LC-MS-MS. This value represents the sum of intracellular protoporphyrinogen IX plus protoporphyrin IX (PPG IX and PP IX, Fig. 1), as the former spontaneously oxidizes to the latter upon extraction. Data represent the mean of three independent experiments. Strains used were SMA1379 (WT, with the *katGΔFG* allele), SMA1383 (*Hpx2⁺*), SMA1399 [*Hpx2 hemH(NI)*] and SMA1161 (ΔhemH).

whereas the *hemH(NI)* strain failed to do so (Fig. 5B). Consequently, the wild-type strain cleared H₂O₂ from the medium; the noninducing mutant did not (Fig. 5C). This phenotype was even more consequential than is apparent from measures of biomass. Figure 5D illustrates that the *hemH(NI)* cultures lost several logs of viability.

The increased sensitivity of *hemH(NI)* strains to H₂O₂ was also apparent in disk diffusion assays (Fig. 6A). For clarity, it was examined in an *ahpF* mutant background, which lacks NADH peroxidase (AhpcF) and therefore relies exclusively upon catalase for H₂O₂ clearance. The *ahpF* strains constitutively induce low-level expression of the OxyR regulon and thus typically display greater H₂O₂ resistance when challenged with a zone-of-inhibition assay (Seaver and Imlay, 2001a), and that effect is apparent in Fig. 6A. Still, the *hemH(NI)* strain showed greater sensitivity than the strain in which *hemH* was inducible. In catalase-deficient cells, the *hemH(NI)* allele had no phenotype. These data indicate that *hemH* induction is necessary to provide heme for KatG activation during H₂O₂ stress.

The accumulation of porphyrins is also potentially toxic *per se*, in part because photoexcited porphyrins can trigger singlet oxygen formation (Miyamoto *et al.*, 1991). That does not appear to be the primary mechanism of poisoning here, as the growth defects that emerged correlated with the failure to scavenge H₂O₂, and they persisted when experiments were performed in the dark.

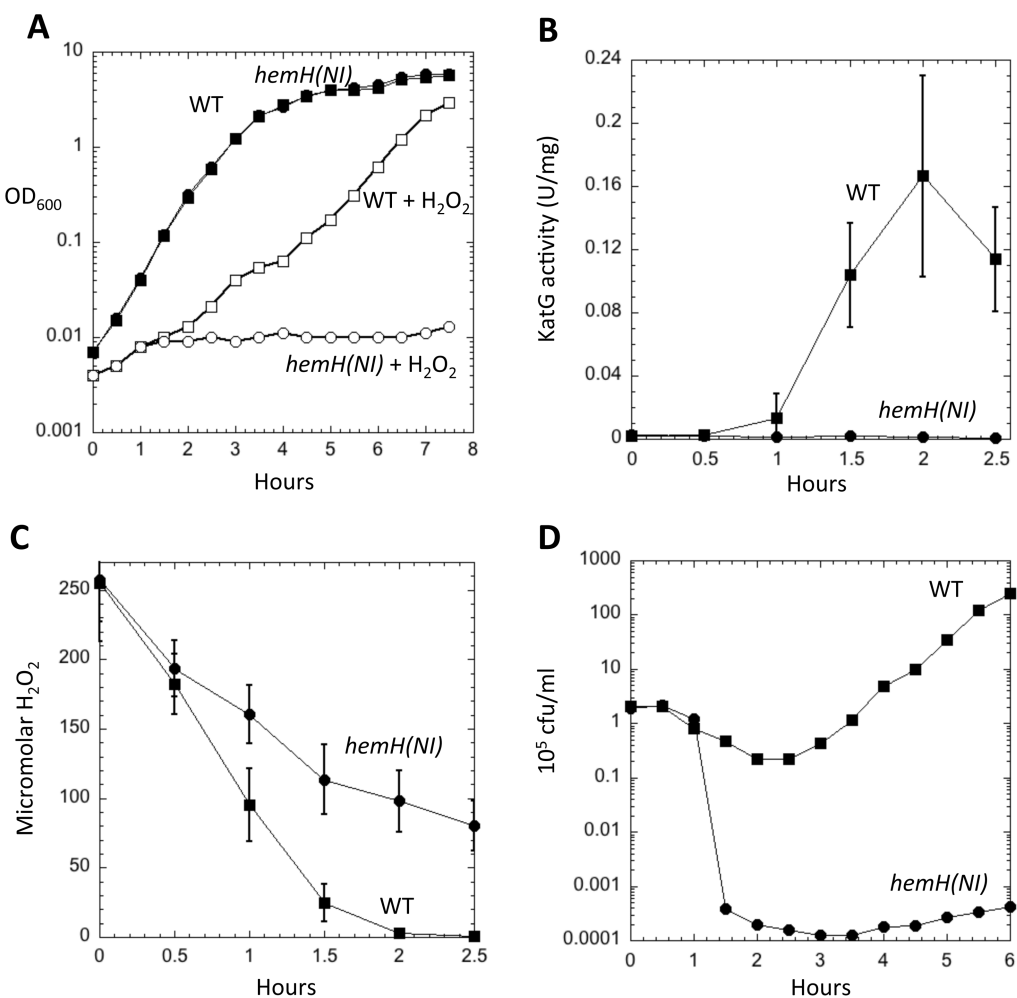


Fig. 5. The induction of *hemH* is critical for resistance to exogenous H₂O₂. At time zero, a bolus of H₂O₂ was added to exponential *hemH*⁺ and *hemH(NI)* cultures in LB medium.

A. Growth.

B. KatG peroxidase activity.

C. Residual H₂O₂ in the medium.

D. Viable cells, as determined by dilution and plating. Note that the time frames differ among panels. Strains were MG1655 (WT) and SMA1035 [*hemH(NI)*] in panels A–C and JI370 ($\Delta ahpF$) and SMA1129 [*hemH(NI) ΔahpF*] in panel D. All data represent the means of three independent experiments.

hemH induction avoids a ferrochelatase bottleneck during iron deficiency

The transcriptomic data offered a clue as to why ferrochelatase had special problems during H₂O₂ stress: the availability of its substrate, ferrous iron, was diminished. Indeed, although KatG activity was deficient when *hemH(NI)* cells were confronted with H₂O₂, it was normal in unstressed *hemH(NI)* cells containing *poxyR2*, with both strains exhibiting 0.4 U mg⁻¹ activity compared with ~0.01 U mg⁻¹ for vector controls (Fig. 7). Thus, it is H₂O₂ per se that demands *hemH* induction, rather than merely heightened flux demand during catalase synthesis.

The depletion of cytoplasmic iron results both from its chemical oxidation to the insoluble ferric form and from the iron-sequestering action of Dps. Several experiments demonstrated that *hemH* induction was important under conditions of iron deficiency. First, a strong growth phenotype emerged even at low H₂O₂ doses when the iron chelator dipyridyl was used to deplete iron from the medium of Hpx2⁻ *hemH(NI)* cultures (Fig. 6B). The need for *hemH* induction was also observed when exogenous H₂O₂ was added to cells that were iron-poor by virtue of mutations in iron importers (Fig. S6). The *hemH(NI)* strain was especially slow to induce KatG activity, with consequent delays in H₂O₂ degradation and growth.

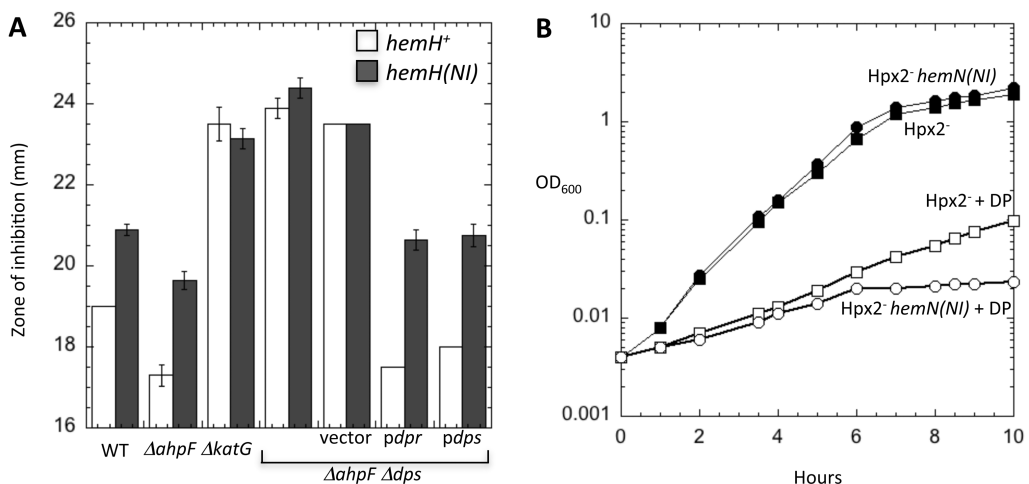


Fig. 6. Induction of *hemH* is critical for H_2O_2 resistance when intracellular iron is sequestered.

A. The *hemH(NI)* allele sensitizes cells only if cells synthesize both catalase and the Dps iron-storage protein. Paper disks presoaked with H_2O_2 were laid onto cells that had been spread onto plates in LB top agar, and zones of inhibition were measured after 24 h.
B. Dipyridyl imposes the need for *hemH* induction even when H_2O_2 levels are low. Cultures in glucose/amino acids medium were aerated at time zero (without exogenous H_2O_2 addition). Where indicated, 0.75 mM of the cell-permeable iron chelator dipyridyl (DP) was included in the medium. For panel A, the strains were MG1655 (WT), SMA1035 [*hemH(NI)*], JI370 ($\Delta ahpF$), SMA1129 [$\Delta ahpF$ *hemH(NI)*], SMA1306 ($\Delta ahpF$ $\Delta katG$), SMA1308 [$\Delta ahpF$ *hemH(NI)* $\Delta katG$], SMA1247 ($\Delta ahpF$ *dps*), SMA1249 [$\Delta ahpF$ *dps* *hemH(NI)*], SMA1274 ($\Delta ahpF$ Δdps with vector), SMA1275 ($\Delta ahpF$ Δdps *dps*), SMA1276 ($\Delta ahpF$ Δdps *dpr*), SMA1277 [$\Delta ahpF$ Δdps *hemH(NI)* with vector], SMA1278 [$\Delta ahpF$ Δdps *hemH(NI)* *dps*], SMA1279 [$\Delta ahpF$ Δdps *hemH(NI)* *dpr*]. For panel B, the strains were SMA1383 (Hpx2⁺) and SMA1399 [Hpx2⁻ *hemH(NI)*]. The data represent three independent experiments.

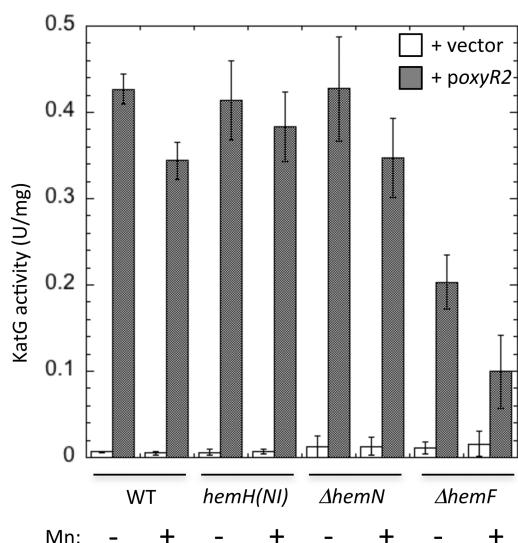


Fig. 7. The induction of *hemF* but not *hemH* is needed to synthesize ample heme in the absence of H_2O_2 stress. Levels of KatG peroxidase activity were measured in strains containing either an empty vector or *oxyR2*. Where indicated, 10 μ M $MnCl_2$ was added to the glucose medium to ensure HemF activation. Strains used were SMA1151 (WT with vector), SMA1149 (WT *oxyR2*), SMA1153 [*hemH(NI)* with vector], SMA1039 [*hemH(NI)* *oxyR2*], SMA1507 ($\Delta hemF$ with vector), SMA1509 ($\Delta hemF$ *oxyR2*), SMA1511 ($\Delta hemN$ with vector), and SMA1513 ($\Delta hemN$ *oxyR2*).

We used disk-diffusion assays to assess the impact of *dps* induction on the ferrochelatase phenotype (Fig. 6A). A *dps* null mutation suppressed the growth inhibition of *hemH(NI)* cells exposed to H_2O_2 . Sensitivity was restored by plasmids overexpressing Dps and Dpr, a Dps homolog from *Streptococcus mutans*, showing that Dps and the ferrochelatase are direct competitors for iron during H_2O_2 stress. These results indicate that several features of H_2O_2 stress collaborate to deplete the iron pools available for insertion of iron into protoporphyrin IX, with the consequence that the critical induction of active catalase can fail. Induction of ferrochelatase is a key mechanism of compensation.

HemF is a second heme biosynthetic enzyme induced by OxyR

The sixth step of the heme biosynthetic pathway, the oxidative decarboxylation of coproporphyrinogen III to protoporphyrin IX, is catalyzed by two isozymes, encoded by *hemN* and *hemF* (Fig. 1). HemN is a SAM-radical enzyme with an iron–sulfur cluster, and the enzyme reduces SAM to methionine and 5'-deoxyadenosine (Layer *et al.*, 2006). In contrast, HemF employs molecular oxygen as an electron acceptor; therefore, HemF is functional only in aerobic environments. HemF is notable because it is a rare *E. coli* enzyme that appears to require manganese as its prosthetic metal (Breckau *et al.*, 2003).

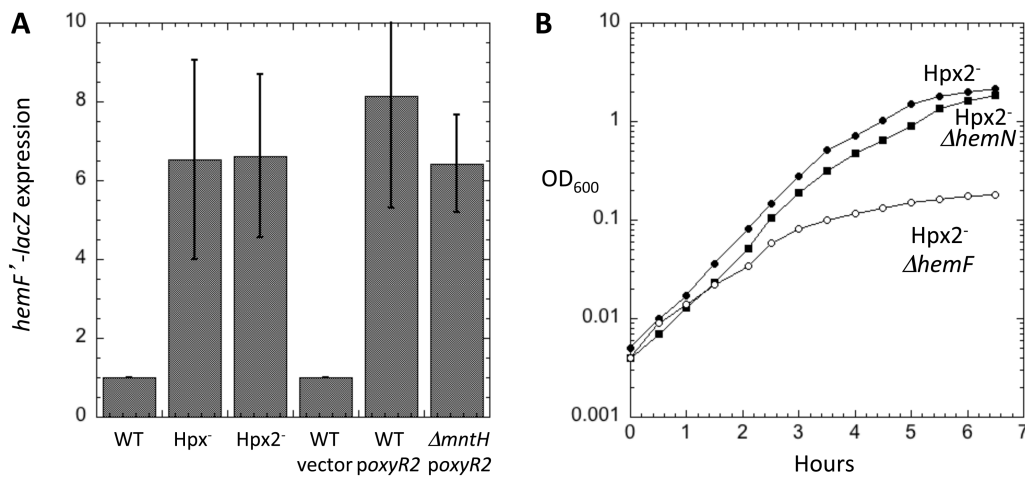


Fig. 8. The induction of *hemF* is necessary for full resistance to H₂O₂.

A. qPCR quantification of *hemF* transcripts in strains growing exponentially in oxic glucose medium. Strains were MG1655 (WT), LC106 (Hpx⁻), SMA1383 (Hpx2⁻), SMA1151 (WT with vector), SMA1149 (WT *poxyR2*) and SMA1431 (*Δmnh* *poxyR2*).

B. Growth of Hpx2⁻ strains (without exogenous H₂O₂) in aerobic LB medium. Strains were LC106 (Hpx⁻), SMA1383 (Hpx2⁻), SMA1539 (Hpx⁻ *ΔhemF*) and SMA1503 (Hpx2⁻ *ΔhemN*).

Prior microarray studies did not note evidence of *hemF* induction during H₂O₂ stress (Zheng *et al.*, 2001; Lee *et al.*, 2009), but Mukhopadyay and Schellhorn reported that the gene was induced 1.8-fold in when cells were exposed to 60 μM H₂O₂ (Mukhopadyay and Schellhorn, 1997). Data suggested that this effect was OxyR dependent. Because wild-type cell cultures rapidly scavenge exogenous H₂O₂, their single-bolus experiments might not have elicited full induction. Our transcriptomic data indicated sixfold induction in Hpx2⁻ cells, and qPCR analysis showed that *hemF* transcripts were induced 6.5-fold in Hpx⁻ cells (Fig. 8A). A similar induction occurred in unstressed cells that harbored the *poxyR2* plasmid. Thus, induction is substantial.

Using 5'-RACE, we found that during routine growth, the *hemF* transcriptional start site is located 243 bp upstream of the *hemF* ORF, within the 3' end of the upstream *amiA* ORF; however, in Hpx2⁻ cells the predominant start site lies 30 bp further upstream, suggesting that OxyR enables RNA polymerase to bind to a new site (data not shown). OxyR binding sites are not easily recognized, and we were unable to locate one by visual inspection. The similarity of induction in catalase-expressing Hpx2⁻ and catalase-free Hpx⁻ strains indicated once again that the gene was not responding to increased heme demand. Because HemF can use manganese as a cofactor, we considered the possibility that *hemF* induction might be coupled to manganese availability, so that the OxyR effect was an indirect consequence of its induction of the MntH manganese importer. However, the *poxyR2* plasmid induced *hemF* as effectively in a *mnh* null mutant as in the wild-type background, indicating that manganese availability does not

cause *hemF* induction (Fig. 8A). We conclude that *hemF* is apparently an authentic member of the OxyR regulon.

HemF supersedes HemN as a coproporphyrinogen III oxidase during H₂O₂ stress

Following the logic of the *hemH* investigation, we tested whether HemF synthesis was important during H₂O₂ stress. Because cytochrome oxidase activity is essential for aerobic growth, a *ΔhemN* *ΔhemF* double mutant that cannot synthesize heme was viable only in anoxic medium, where *E. coli* ferments. Both of the *ΔhemF* and *ΔhemN* single mutants were able to grow at normal rates in the presence of oxygen, indicating that either protein is sufficient for heme synthesis in unstressed cells (Fig. S7). However, during H₂O₂ stress, HemN is no longer adequate. In oxic glucose medium, an Hpx2⁻ *ΔhemF* strain exhibited a mild growth defect relative to an Hpx2⁻ *hemF*⁺ strain (Fig. S8). This phenotype was more pronounced in LB medium, where catabolism is more dependent upon respiration (Fig. 8B). It was fully complemented (Fig. S9). Furthermore, in the Hpx2⁻ background, a *ΔhemF* mutation diminished KatG peroxidase and cytochrome oxidase activities, whereas a *ΔhemN* mutation was without effect (Fig. 9). The cytochrome oxidase defect was lessened in *ΔkatG* deletion strains (Hpx⁻, compared with Hpx2⁻), wherein heme demand is reduced. This pattern was pronounced in nonfermentative LB medium (Fig. S10). Manganese supplementation elevated the activities of heme-containing enzymes in all strains except those containing *ΔhemF* mutations, consistent with its role in activating HemF (Fig. 9). These data all indicate that during H₂O₂

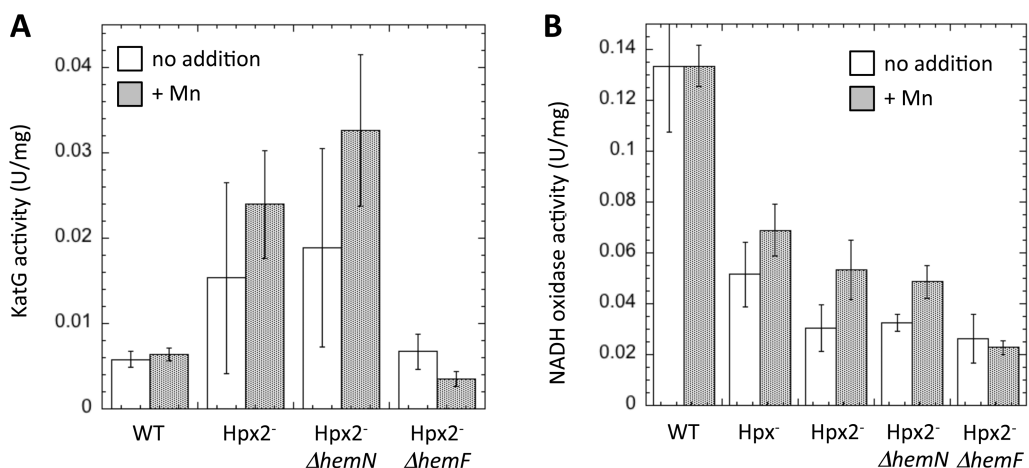


Fig. 9. Induction of *hemF* is necessary for the efficient activation of KatG during H₂O₂ stress. Peroxidase (A) and NADH oxidase (B) activities were determined for cells growing in aerobic glucose medium. Where indicated, the medium was supplemented with 10 µM MnCl₂. Data represent the mean of three independent experiments. The strains were SMA1379 (WT, with *katGΔFG* allele), SMA1383 (Hpx²⁻), SMA1505 (Hpx²⁻ ΔhemN) and SMA1503 (Hpx²⁻ ΔhemF).

stress, the induced mangano-enzyme HemF becomes the critical coproporphyrinogen III oxidase.

Measurements of intracellular coproporphyrinogen III pools confirmed this interpretation (Fig. 10). The pools were undetectably small in both wild-type and Hpx²⁻ strains. The ΔhemN mutation alone had little or no effect, either in unstressed or Hpx²⁻ strains. However, inside Hpx²⁻ ΔhemF mutants, this porphyrin rose to a high level.

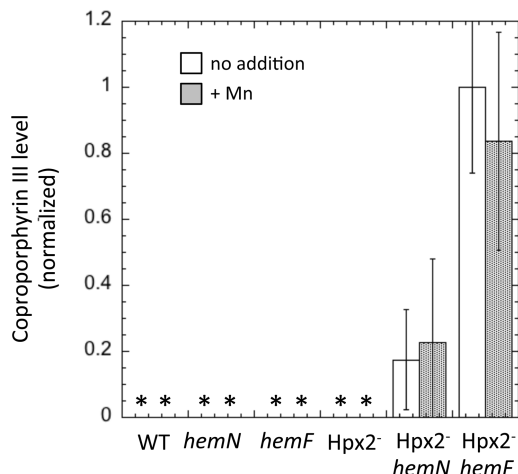


Fig. 10. During H₂O₂ stress coproporphyrinogen III accumulates unless *hemF* is induced. Cells were grown in aerobic glucose medium, and their coproporphyrinogen III content was determined by the LC-MS-MS quantitation of coproporphyrin, the oxidation product of coproporphyrinogen. Asterisks (*) indicate that values fell below the detection limit on all three biological replicates. Where indicated, the medium was supplemented with 10 µM MnCl₂. Data represent the mean of three independent experiments. Strains used were SMA1379 (WT, with the *katGΔFG* allele), SMA1499 (ΔhemN), SMA1497 (ΔhemF), SMA1383 (Hpx²⁻), SMA1505 (Hpx²⁻ ΔhemN) and SMA1503 (Hpx²⁻ ΔhemF).

Because it employs a [4Fe-4S] cluster, we wondered whether the inadequacy of HemN was due to its poisoning by H₂O₂. However, unstressed *poxyR2* cells that overexpress the OxyR regulon – and, with it, the KatG protein – were also unable to fully charge the enzyme using HemN alone (Fig. 7). Thus, basal levels of HemN cannot support a high pathway flux even in the absence of H₂O₂ stress, whereas HemF is able to do so. The induction of *hemF* by OxyR might be an important element in ensuring that HemF titers are sufficient, but we were unable to test this idea through promoter manipulation, as this promoter is located within *amiA*, an important cell-wall enzyme. Of course, the fact that HemN titers are inadequate for high flux even without H₂O₂ stress does not rule out the possibility that HemN is additionally vulnerable to H₂O₂ (see Discussion).

Mutants lacking HemF cope poorly with H₂O₂ stress

The preceding experiments were conducted in Hpx²⁻ backgrounds in which KatG was unable to degrade H₂O₂. However, problems with heme synthesis will generate the strongest phenotypes under conditions in which catalase activity actively detoxifies the environment. Indeed, in wild-type *katG⁺* backgrounds, ΔhemF mutants were unable to cope with exogenous H₂O₂ (Fig. 11A and B). In contrast, the ΔhemN strain that could express *hemF* was able to perform as well as the wild-type strain. Measurements of the viability of strains lacking the NADH peroxidase (AhpCF) – which therefore relied exclusively on the catalase for H₂O₂ degradation – revealed that *hemF* was needed not only to avoid cell stasis but also to avoid death. A similar result was observed in zone-of-inhibition experiments, in which the bacteria encounter H₂O₂ as a

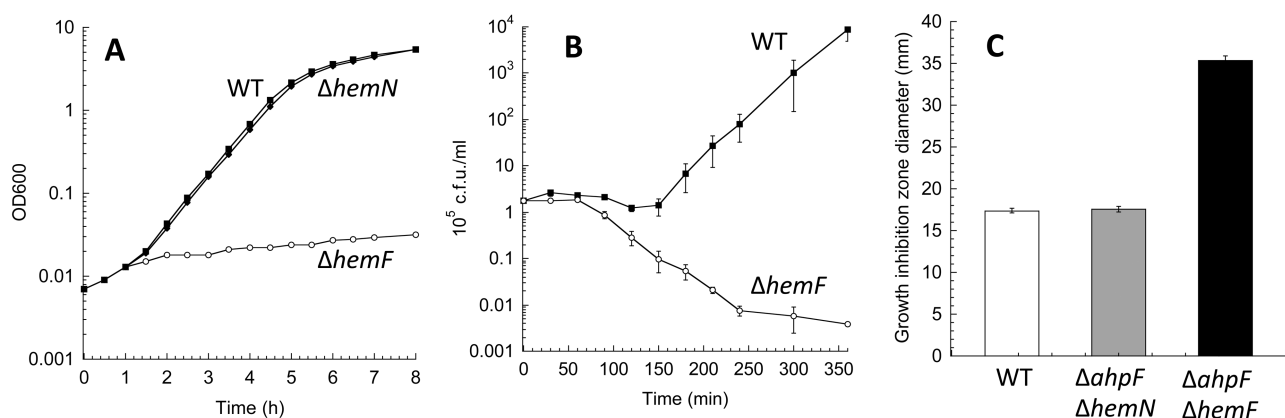


Fig. 11. The HemF isozyme is necessary for resistance to exogenous H₂O₂.

(A–B). At time zero anoxic cultures were diluted into oxic LB medium containing 0.3 mM (A) and 0.5 mM (B) H₂O₂. Growth (A) and viability (B) were monitored.

C. Paper disks pre-soaked with H₂O₂ were laid onto cells that had been spread onto plates in LB top agar, and zones of inhibition were measured after 24 h. Data are representative of three independent experiments. Strains used were MG1655 (WT), SMA1497 (ΔhemF) and SMA1499 (ΔhemN) in panels A and B and MG1655 (WT), SMA1521 ($\Delta\text{ahpF}\Delta\text{hemN}$) and SMA1519 ($\Delta\text{ahpF}\Delta\text{hemF}$) in panel C.

time-dependent gradient of increasing concentration (Fig. 11C). This experimental design optimizes the opportunity for induction. In sum, during H₂O₂ stress HemF is needed to achieve high heme synthetic fluxes, and rapid heme synthesis is needed to maintain cell fitness. HemN, an iron–sulfur enzyme that is adequate during routine growth, is insufficient in this situation.

Discussion

Oxidative stress is perhaps the most common threat experienced by organisms in natural habitats. Variability in oxidant resistance shapes the biota in such clear ways that a basic description of a microorganism starts with its classification as an aerobe, microaerophile or anaerobe. Still, our understanding of the mechanisms by which oxidants damage cells is not yet complete, nor do we have a full command of the defensive strategies by which organisms defend themselves.

Progress has been greatly facilitated by analysis of the bacterial OxyR response, one of the first defensive regulons that was defined using contemporary transcriptomics. In this study, RNA-seq data emphasized that H₂O₂ stress creates a global crisis in iron utilization and that this problem ramifies to the synthesis of heme as a cofactor for catalase. Although catalase provides a primary defense against H₂O₂, the function of the two iron-requiring enzymes in that pathway becomes problematic, and the OxyR response has evolved to remedy the situation.

A crisis in iron availability: induction of HemH protein

All the well-characterized injuries produced by H₂O₂ start with its oxidation of iron: DNA damage (Park *et al.*, 2005),

inactivation of [4Fe-4S] dehydratases (Jang and Imlay, 2007) and mononuclear iron enzymes (Sobota and Imlay, 2011; Anjem and Imlay, 2012; Sobota *et al.*, 2014), inhibition of the lsc system (Jang and Imlay, 2010), and derepression of the Fur regulon (Varghese *et al.*, 2007). All these reactions are derivatives of the basic Fenton reaction, where inner-sphere electron transfer from ferrous iron to H₂O₂ produces a hydroxyl radical. This species is itself toxic, causing the covalent oxidation of DNA and polypeptide residues.

The fact that H₂O₂ damage derives almost exclusively from iron might seem surprising, because the cell contains several biomolecules – including thiols, flavins and quinones – with a lower reduction potential. However, the d-orbitals of transition metals like iron and copper lower the activation energy of H₂O₂ reduction by stabilizing the radical that is formed, as evidenced by the fact that the Fenton reaction produces a ferryl radical, rather than a free hydroxyl radical, as the immediate product (Imlay *et al.*, 1988; Rush *et al.*, 1990). Because *E. coli* systematically excludes copper from its cytoplasm (Dupont *et al.*, 2011), ferrous iron is left behind as the biomolecule most reactive with H₂O₂. Thus, the cellular adaptation to H₂O₂ is centered around minimizing the amount of intracellular ferrous iron. Ferritins keep intracellular pools at moderate levels during routine growth (Touati *et al.*, 1995; Andrews *et al.*, 2003), and during periods of H₂O₂ stress the induction of Dps drives them lower (Ilari *et al.*, 2002; Park *et al.*, 2005).

The problem with this arrangement is that iron pools are needed for the activation of mononuclear iron enzymes, iron–sulfur proteins and heme proteins. In Hpx⁺ cells the derepression of the Fur regulon indicates that the combination of Dps synthesis and chemical iron oxidation drives ferrous levels quite low. Previous works showed some

strategies that the H₂O₂-stressed cell uses to sustain iron-enzyme activation. The induction of the MntH importer rescues the mononuclear enzymes, apparently by providing manganese as a substitute for their iron atoms (Anjem *et al.*, 2009; Sobota and Imlay, 2011; Anjem and Imlay, 2012). Induction of Suf enables cluster synthesis to continue, as the Suf machinery can function effectively even when iron levels drop too low for the standard Isc machinery (Jang and Imlay, 2010).

However, heme synthesis is potentially the most problematic of all. When moderate levels of H₂O₂ inactivate the NADH peroxidase (Ahp), the induction of catalase is the sole way to drive the H₂O₂ levels back down (Seaver and Imlay, 2001a). The data indicate that the two iron-dependent steps of heme synthesis – coproporphyrinogen III oxidation and protoporphyrin IX metallation – are both at risk, and the inductions by OxyR of ferrochelatase and HemF are critical adaptations. The problem is not simply the increase in heme demand. Recent ribosome profiles of glucose-grown *E. coli* (Li *et al.*, 2014) indicate that in unstressed cells KatG represents only 7–10% of the heme proteins (Table S3); thus, its 14-fold induction during H₂O₂ stress approximately doubles the heme demand of the cell. Most cofactor biosynthetic pathways are synthesized with excess capacity and, as we discovered for heme, show little evidence of product-dependent feedback regulation at the transcriptional level. (This statement applies to thiamine, pyridoxamine, flavin, pantothenate, lipoate, quinone and folate synthesis, but not to nicotinamide, which cells require at millimolar rather than micromolar levels.) We presume that this excess capacity explains why catalase induction does not require the induction of the other heme biosynthetic genes. In fact, an exception that proves the rule is the observation that in *Bacillus subtilis* many heme genes belong to its H₂O₂-response regulon, as this bacterium induces catalase to such enormous levels that in *perR* mutants it rises to 10% of the total cell protein (Faulkner *et al.*, 2012).

Thus, the induction of ferrochelatase is apparently a strategy to sustain heme synthesis despite the depletion of the ready pool of ferrous iron, the ferrochelatase substrate. Notably, *E. coli* does not appear to use frataxin or any analogous chaperone to protect a supply of iron from Dps and H₂O₂. Disk diffusion assays revealed that a null mutation of a frataxin homolog, encoded by *cyaY*, did not have any impact on the H₂O₂ sensitivity of *hemH(NI)* strains (data not shown). Moreover, $\Delta cyaY$ mutants did not exhibit defects in iron-enzyme activities, either in wild-type or Hpx[−] backgrounds.

Dps puts a strain on iron metabolism when it sequesters the iron pool, and several features of the protein suggest that cells are quick to deactivate it when the H₂O₂ threat has passed. First, *in vitro* experiments indicate that Dps uses H₂O₂ as a co-reactant when Dps oxidizes and stores the

iron (Chiancone and Ceci, 2010). If so, once the H₂O₂ is gone, Dps should stop scavenging iron. Second, the expression of *dps* can be blocked by the manganese-bound form of the MntR repressor (Yamamoto *et al.*, 2011). This arrangement suggests that the primary purpose of iron sequestration is to ensure that manganese, rather than iron, occupies the divalent-metal binding sites in mononuclear proteins. Indeed, Hpx[−] *dps* and Hpx[−] *mntH* mutants both suffer incapacitating levels of protein oxidation due to Fenton chemistry, and this damage can be avoided by manganese supplements (Anjem *et al.*, 2009). As soon as sufficient manganese has been imported, restrictions on iron content can be relieved. Finally, the Dps protein has a terminus that targets it for rapid turnover by the ClpXP protease (Stephani *et al.*, 2003); thus, once H₂O₂ has been scavenged, OxyR-dependent Dps synthesis ends, and extant Dps protein is quickly degraded. The OxyR response is an interesting example in which a cellular adaptation to stress creates secondary problems of its own, which in turn have been minimized by multilayered control features.

Why is HemF induced in place of HemN during H₂O₂ stress?

The coproporphyrinogen III oxidase of *E. coli* is unique among the heme synthetic enzymes in that its activity can be supplied by either of two isozymes, HemN and HemF. All other heme synthetic steps depend on single enzymes. We construe HemN as the housekeeping enzyme because it can function in anoxic as well as oxic habitats, in contrast to the oxygen-dependent HemF, and because HemN is quantitatively fourfold more abundant even under aerobic conditions (Li *et al.*, 2014). Similarly, HemN appears to be the primary coproporphyrinogen III oxidase in aerobic *Pseudomonas aeruginosa* despite the presence of HemF (Rompf *et al.*, 1998).

Our data showed that HemN becomes inadequate during periods of H₂O₂ stress. Why? Several nonexclusive explanations are plausible. First, this step might simply be rate-limiting for the pathway, as it has been reported to be in mammals during erythroid differentiation (albeit with a distinct enzyme) (Severance and Hamza, 2009). This would not explain, however, why an isozyme of a different constitution is induced during H₂O₂ stress. Second, HemN is an S-adenosyl methionine- (SAM-) radical enzyme and therefore relies upon a [4Fe-4S] cluster for function. Indeed, its synthesis is repressed in iron-starved cells (Troup *et al.*, 1995). Because H₂O₂ depletes iron and directly interferes with Isc-dependent cluster synthesis, HemN activation might be difficult in environments where H₂O₂ stress is chronic.

Escherichia coli expresses eight other SAM-radical enzymes – for thiamine, lipoate and biotin synthesis, RNA

modification, and glycyl-radical-enzyme activation. One might expect their synthesis to become problematic during H₂O₂ stress, too, but unlike HemN they do not have compensatory isozymes. Presumably the key difference is that during H₂O₂ stress a slow-down in heme synthesis can be catastrophic, because of its role in catalase activation, whereas impedance of these other pathways is less consequential.

The other vulnerability of HemN might stem from the physical exposure of its [4Fe-4S] cluster. Iron–sulfur dehydratases are poisoned by H₂O₂ because it directly oxidizes their clusters to unstable valences. The HemN cluster can be similarly accessed by small solutes, as evidenced by the ability of soft metals to disrupt it *in vivo* (Azzouzi *et al.*, 2013; Djoko and McEwan, 2013), and so it seems possible that H₂O₂ might directly bind and oxidize it. More work is needed to test this idea. In any case, the induction of a manganese isozyme during oxidative stress would avoid all these problems. This adaptation mirrors the induction of the manganese-dependent superoxide dismutase, rather than the housekeeping iron enzyme, when oxidants activate the SoxRS system (Fridovich, 1986). The activation of HemF constitutes a second reason for MntH induction by OxyR.

Finally, it is intriguing that the heme synthetic pathways in eukarya exclusively employ HemF rather than HemN (Cavallaro *et al.*, 2008). This arrangement, too, mirrors that of superoxide dismutases: eukaryotic mitochondria contain a manganese isozyme but not an iron one. They have also dispensed with the iron–sulfur-dependent fumate reductase, routinely using a cluster-free fumarate C isozyme, which *E. coli* induces only when oxidative stress is sensed. In these regards eukarya seem to constitutively express the defensive strategies that *E. coli* resorts to only under oxidative duress. And at the extreme of the spectrum lie lactic acid bacteria, which routinely generate millimolar concentrations of H₂O₂ as a by-product of central metabolism (Pericone *et al.*, 2003). These bacteria potentially profit if the H₂O₂ poisons their competitors. To avoid toxicifying themselves, they have eschewed the dehydratases that contain labile [4Fe-4S] clusters, they routinely import millimolar levels of manganese that probably cofactor their mononuclear enzymes in place of iron and they do not synthesize heme at all (Bauereder and Hederstedt, 2013). The adaptive strategies of *E. coli* apparently mimic the evolutionary strategies by which organisms cope with oxidative stress.

The global view: transcriptional responses to physiological levels of H₂O₂

We examined the transcriptional response when *E. coli* contended with the ~1 μM H₂O₂ that accumulates in Hpx[−] mutants. The use of this strain is a convenient way of

imposing a degree of chronic H₂O₂ stress that slightly exceeds the trigger for OxyR activation. Wild-type (scavenger-proficient) cells would experience a similar intracellular dose when they are exposed to ~5 μM extracellular H₂O₂, which might be found in a variety of natural habitats. Notably, calculations suggest that phagocytosed bacteria confront steady-state levels of H₂O₂ similar to this (Winterbourn *et al.*, 2006; Imlay, 2009; Burton *et al.*, 2014).

The overall picture was surprising clear: of the 50 operons that responded most strongly to H₂O₂ in this study, all but two are known members of the OxyR, SOS or Fur regulons. The data provide an interesting comparison to the microarray results of Zheng and Storz (Zheng *et al.*, 2001). Their study detected most of the OxyR-controlled genes, but it also detected the induction of OxyR-independent genes that do not overlap at all with our OxyR-independent gene set. The key difference stems from the experimental protocol. As Zheng and Storz recognized, the millimolar dose of H₂O₂ that they used would rapidly activate OxyR, but it would also be sufficient to block cell growth and to oxidize transcription factors that are not significantly affected by micromolar concentrations. Another difference is that our Hpx[−] strain was cultured for many generations prior to RNA harvesting, and so the RNA-seq analysis also detected cellular responses to progressive DNA damage accumulation (the SOS response) and to the impact that OxyR-driven adaptations imposed upon iron metabolism (Fur derepression). The requirement for *hemH* and *hemF* induction apparently results from the latter disturbance of iron metabolism.

The genes that exhibit strong H₂O₂-sensitive phenotypes (*dps*, *fur*, *yaaA*, *mnh*, *sufABCDSE*, *katG*, *ahpCF*, *xthA*, *recA*, *hemH* and *hemF*) were all induced in the Hpx[−] mutants. Thus, an interesting note is that many genes that have been hypothesized to play key roles in oxidative stress were *not* induced (Table S6). These include *soxS* and the regulon it controls, which fits with the observation that the SoxR protein is not easily oxidized by physiologically doses of H₂O₂ (Manchado *et al.*, 2000; Gu and Imlay, 2011). The list also includes genes encoding methionine sulfoxide reductases (*msrA* and *msrB*), periplasmic defensive systems (*degP*, *cpxA*, *dsbB*, *ompF* and *skp*), the cysteine and glutathione synthetic pathway (*cysA*, *cysJ*, *gshA*, *gshB*, etc.), the Hsp33 disulfide-activated chaperone (*hsfO*), RpoS-dependent defensive enzymes (*sodC*, *cfa*, *bolA*, etc.) and the *mutT/mutM/mutY* troika that collectively avoid the effects of the incorporation of 8-oxo-dGTP into DNA. The fact that the cell has not evolved to increase the titers of these proteins suggests that the injuries that they address may not be generated in significant amounts during physiological H₂O₂ stress. Indeed, we have not observed growth defects when most of these genes are deleted from Hpx[−] cells. We suspect that these proteins fix injuries that are generated in other ways.

Nevertheless, more work must be done to make this conclusion definitive.

Moderate activation of the SOS regulon was evidenced in the Hpx⁻ strains by induction of the cryptic e14 bacteriophage genes, *recN*, *sulA*, *tisB*, *umuCD*, *dinB*, *recA* and other regulon members (Table S1). The SOS response has usually been studied as a recovery phenomenon during the period after exposure to DNA-damaging agents, such as UV radiation; however, in the H₂O₂-stressed cells, the response was detected while growth and DNA replication continued. *Hpx ΔrecA* mutants, which cannot activate the SOS response, gradually die in aerobic medium (Park *et al.*, 2005), indicating that potentially lethal amounts of DNA damage occur throughout the full population and that the SOS response is a key element in H₂O₂ resistance. The idea that SOS induction does not always interrupt replication and cell division fits the model that the response is a graded one. Members of the regulon differ in how easily they are induced by DNA damage, apparently in accordance with the numbers and positions of their LexA binding sites (Courcelle *et al.*, 2001). The low-grade stress suffered by our Hpx⁻ strains did not rise to the level of blocking cell septation, for example. The standard stresses that have been used to study the SOS response – intense UV radiation, DNA-damaging chemicals and topoisomerase inhibitors – are unlikely to be the real-world stresses that the SOS system evolved to confront. It may be that oxidative lesions are a natural source of SOS induction. This thought is supported by parallels between the SOS response that we observed and that of *Neisseria gonorrhoeae*. *N. gonorrhoeae* maintains a small SOS regulon whose LexA-type repressor appears to be directly deactivated when H₂O₂ oxidizes a sulfhydryl residue (Schook *et al.*, 2011), a mechanism similar to the activation of OxyR. Furthermore, the primary member of the *N. gonorrhoeae* regulon is *recN* – the SOS-controlled repair enzyme that was most strongly induced in our Hpx⁻ cells. Thus, micro-molar H₂O₂ might be a predominant activator of SOS in natural environments.

The *psp* and *norRVW* genes were strongly induced despite lying outside of the OxyR, SOS or Fur regulons. The 'phage shock protein' system senses membrane stress (Jovanovic *et al.*, 2014), but the physical nature of the signal during H₂O₂ accumulation is unclear and is worthy of further investigation. NorW and NorV comprise a two-component nitric oxide reduction system that has no obvious role during H₂O₂ stress. Their induction may be an accidental consequence of the oxidation of the iron cofactor of NorR, the transcription factor that activates transcription of the three *nor* genes (Tucker *et al.*, 2008). NorR employs a ferrous iron atom to sense nitric oxide by directly binding it; in Hpx⁻ cells, however, H₂O₂ is likely to oxidize the iron atom, and the resultant ferryl radical would be expected to further oxidize its coordinating

cysteine residue, as with other mononuclear iron proteins (Anjem and Imlay, 2012; Sobota *et al.*, 2014). If so, the induction of this operon may be one more example of the impact of adventitious Fenton chemistry.

Finally, a recent report suggested that YchF, an ATPase, is a negative regulator of the oxidative stress response and is repressed by OxyR (Wenk *et al.*, 2012). We did not observe any impact of H₂O₂ stress upon *ychF* expression. Furthermore, although YchF was proposed to directly bind and inhibit KatG in unstressed cells, a *ΔychF* mutant exhibited the same activity as did a wild-type cell (data not shown), in contrast to that previous report. It is not clear whether some aspect of growth condition influences the behavior of YchF.

Experimental procedures

Reagents

D-glucose and Tris base were purchased from Fisher Scientific; ethylenediaminetetraacetic acid disodium salt dehydrate (EDTA) and xylolol orange disodium from Fluka; Amplex Red from Molecular Probes; ECL Western Blotting Detection Reagents from Amersham; glacial acetic acid from J.T. Baker Chemicals; and 6 mm blank paper disks from Beckton, Dickinson and Co. Acid-hydrolyzed casamino acids (Hy-Case Amino), L-amino acids, chloramphenicol, ampicillin, 2-(N-morpholino)ethanesulfonic acid (MES), ethyl acetate, sorbitol, 2,2'-dipyridyl, o-nitrophenyl-β-D-galactopyranoside (ONPG), o-dianisidine dihydrochloride, NADH, potassium ferricyanide, potassium cyanide, ferrous ammonium sulphate hexahydrate, manganese (II) chloride tetrahydrate, 30% H₂O₂, type II horseradish peroxidase and horseradish peroxidase-conjugated anti-rabbit goat IgG were obtained from Sigma-Aldrich. Rabbit serum containing anti-KatG IgG was a kind gift of Dr. Peter Loewen. Rabbit serum containing anti-HemA IgG was purchased from Pierce Biotechnology.

Growth conditions

Anoxic growth was performed in an anaerobic glove box (Coy Laboratory Products) under an atmosphere of 85% nitrogen, 10% hydrogen and 5% carbon dioxide. Aerobic cultures were grown in the open laboratory with vigorous shaking. All the cultures were incubated at 37°C. For all the experiments, overnight cultures were diluted in the appropriate medium to OD₆₀₀ = 0.005 and grown for at least four generations to reproducibly establish log-phase physiology. To prevent DNA damage, oxygen-sensitive strains were precultured anoxically. Mid-log cells were then diluted into fresh aerobic medium to an OD₆₀₀ = 0.005–0.02 (as specified below) for subsequent experiments. OD₆₀₀ was used to monitor cell growth. Standard glucose medium consisted of minimal A salts (Miller, 1972) plus 0.2% glucose, 5 mg ml⁻¹ thiamine, 1 mM MgSO₄, 0.5 mM aromatic amino acids and 0.5 mM histidine. Histidine was supplied because the parental strain (MG1655) is a histidine bradytroph under anoxic conditions, and aromatic amino acids were supplied because aromatic

biosynthesis is inhibited by the low doses of H₂O₂ that accumulate in the oxic media of Hpx⁺ strains (Sobota *et al.*, 2014). Glucose/amino acids medium contained 0.2% casamino acids and 0.5 mM tryptophan in place of aromatic amino acids and histidine. LB contained (per liter) 10 g tryptone, 10 g NaCl and 5 g yeast extract. Glucose/amino acids or LB media were used in experiments involving high doses of H₂O₂, which otherwise blocks branched-chain biosynthesis.

Bacterial strains and strains construction

The strains used in this study are listed in Table S4. The construction of all the oxygen-sensitive strains was performed under anaerobic conditions to ensure that suppressor mutations were not selected during outgrowth. Null mutations were created by using the λ Red recombinase method (Datsenko and Wanner, 2000). The mutations were moved to the desired background by P1 transduction (Miller, 1972) and confirmed by polymerase chain reaction (PCR) analysis. When necessary, the resistance marker was removed – leaving a *fip* scar sequence – by transformation with pCP20, followed by removal of the temperature-sensitive plasmid (Datsenko and Wanner, 2000).

The chromosomal *hemH(NI)* allele had much of the OxyR binding site removed and replaced with the *fip* scar sequence. This mutation was achieved by the λ Red recombinase method and confirmed by PCR analysis. The genomic region comprising –204 to –36 from the start site, corresponding to bases 497051–497220 of *E. coli* genome, was removed in the *hemH(NI)* mutant allele. This deletion removed the majority of the OxyR binding cassette, which is located between –63 and –25 from the start site (Zheng *et al.*, 2001), and did not modify the overlapping –35 promoter region or the 5' UTR of the transcript.

Single-copy *lacZ* transcriptional fusions to *hemH*, *hemH(NI)* and *hemA* promoter regions were integrated into the λ attachment site, thereby leaving intact the native genes (Hasan *et al.*, 1994; Haldimann and Wanner, 2001). The promoter regions were PCR amplified using 5'-TATATACTGCAGATT CGAAAGCGCGACGGAC-3' and 5'-ATATATGAATTCCAT TACCGCCTTATCGATT-3' for *hemH*, 5'-TATATACTGC AGAAAAATCCTCGGCTAATTG-3' and 5'-ATATATGAAT TCCATTACCGCCTTATCGATT-3' for *hemH(NI)*, and 5'-TATATACTGCAGGGGTATAGTGATGACAAGTCC-3' and 5'-ATATATGAATTCCATGTCTGCGGGAAATAATAC-3' for *hemA*. All the primer pairs were designed with PstI and EcoRI recognition sites. The promoter regions were inserted before the *lacZ* ORF in the pAH125-derivative CRIM plasmid pSJ501, where the chloramphenicol cassette permits anaerobic selection. The resulting plasmids were confirmed by restriction analysis and sequencing. The constructs were then integrated into the chromosome at the λ attachment site by the integrase provided by pINT-ts, and they were then transduced into appropriate strains. When necessary, the chloramphenicol resistance cassette, which is flanked by *fip* sites, was subsequently removed by means of pCP20.

Plasmids and plasmid construction

The plasmids used in this work are described in Table S4. The *hemF* ORF was PCR amplified from *E. coli* MG1655

chromosome using the forward primer 5'-TATAGAATTG CACGGCGGGCGTTTCGTCAG-3' and the reverse primer 5'-TATAAGCTTATCAGCGGATGCGGGAGTGG-3'. The primers were designed to include EcoRI and HindIII recognition sites. The *hemF* ORF was inserted into the pBR322 vector, generating the pSM16 plasmid.

Illumina RNA-sequencing

Anoxic precultures of three independent isolates of each strain were grown until exponential phase (OD₆₀₀ ~ 0.1–0.15). Cells were centrifuged 5 min at 7000 × g, and pellets were resuspended in fresh oxic medium to obtain an initial OD₆₀₀ ~ 0.005. Cultures were incubated aerobically with vigorous shaking until they reached an OD₆₀₀ ~ 0.1–0.15. Total RNA was isolated from cells by hot phenol extraction. Briefly, 1.6 ml (2 × 800 µl) of each culture was mixed with preheated phenol-water and fresh 8× lysis solution (20 mM Na-acetate, pH 5.2, 0.5% SDS, 1 mM EDTA, pH 8.0 in DEPC water) and incubated × 15 min at 65°C with vigorous shaking. After centrifugation at 13 000 × g at 10 min at RT, the top layer was transferred to clean Eppendorf tubes containing 700 µl of phenol-chloroform. The phenol-chloroform extraction was repeated twice. The upper aqueous layer was transferred into clean Eppendorf tubes containing 1.3 ml EtOH and incubated 90 min on dry ice. After centrifugation at 13 000 × g at 10 min at 4°C, the supernatants were discarded, and the RNA pellets were rinsed with 500 µl 75% EtOH. The precipitated RNA pellets were air dried and resuspended in 40 µl RNase free TE buffer (10 mM Tris pH 7.0, 1 mM EDTA). Contaminating genomic DNA was removed from the isolated RNA samples by DNase treatment using RNase-free DNase I (New England Biolabs) according to the manufacturer's instructions. The construction of libraries from mRNA and sequencing on the HiSeq2000 were performed by the University of Illinois Biotechnology Center. Briefly, ribosomal RNA was removed from total RNA with the RiboZero Bacteria kit from Epicentre/Illumina. The RNAseq libraries were prepared with Illumina's 'TruSeq Stranded RNAseq Sample Prep kit'. The libraries were pooled, quantified by qPCR and sequenced on one lane for 101 cycles from one end of the fragments on a HiSeq2000 using a TruSeq SBS sequencing kit version 3. Reads 100 nt in length were generated, and Fastq files were produced with the software Casava 1.8.2 (Illumina). RNA-Seq reads were aligned with the genome of *E. coli* MG1655 to generate gene counts that were used for differential gene expression analysis, which was performed by the Bioinformatics unit.

Quantitative real-time PCR

All studies were performed upon cells that had been carefully cultured to the point of exponential growth. For qPCR measurements of gene expression, exponentially growing anaerobic precultures were diluted into fresh oxic medium to OD₆₀₀ = 0.005 and grown with vigorous shaking until cells reached an OD₆₀₀ ~ 0.1–0.15. Two milliliters of each culture were mixed with two volumes of RNA-protect bacterial reagent (Qiagen) and incubated 10 min at room temperature. RNA was extracted from cells with the RNeasy minikit (Invit-

rogen) following the manufacturer's instructions. Contaminating genomic DNA was removed by the isolated RNA samples by DNase treatment using RNase-free DNase I (New England Biolabs) according to the manufacturer's instructions. Dilutions (1/10) of the RNA samples were PCR amplified. The lack of product visualized by gel electrophoresis confirmed the absence of contaminating genomic DNA. One microgram of the DNA-free RNA samples was used to synthesize cDNA with the iScript cDNA Synthesis Kit (BioRad) according to the manufacturer's instructions. Gene expression of *hemF* and *hemH* was analyzed using the primers listed in Table S5. Expression was normalized to the signal of the *rrsG* gene (16S ribosomal RNA). PCR amplifications were performed using iQ SYBR® Green Supermix (BIORAD) according to the manufacturer's instructions. Briefly, a qPCR reaction consisted of a mixture of 10 µl iQ SYBR® Green Supermix (2×), 300 nM forward and reverse primer, 2 µl of 1/10 dilution of the cDNA samples, and H₂O were combined to reach a final volume of 20 µl. PCR was carried out in a MasterCycler ep realplex machine (Eppendorf) as follows: 3 min at 95°C, 40 cycles of 15 s at 95°C, 30 s at 60°C and 30 s at 72°C. A final melt curve analysis from 55°C to 90°C with 0.5°C increments every 2 s was performed to confirm the presence of single amplicates.

5'RLM-RACE

5' RNA ligase-mediated rapid amplification of cDNA ends (RLM-RACE) was performed using First Choice RLM-RACE kit (Ambion) following the manufacturer's indications. RNA isolated from wild-type and Hpx2⁻ cells for the qPCR analysis (0.5 µg) was treated with the tobacco acid pyrophosphatase (TAP) to remove the phosphate from full-length mRNA. The monophosphate mRNA was ligated to the 5' RACE adapter and retro-transcribed to cDNA by using iScript cDNA Synthesis Kit (BioRad) according to the manufacturer's instructions. Two subsequent nested PCRs were performed using the 5'RACE outer 5'-GCTGATGGCGATGAATGAACACTG-3' and inner 5'-CGCGGATCCGAACACTGCGTTGCTGGC TTTGATG-3' adapter forward primers and the gene-specific 5'-AGTCGAAGCCACCGCCAAAC-3' and 5'-ATTACGCAA CACCCGACTAC-3' reverse primers for the outer and inner 5' PCR respectively. The PCR reactions were electrophoresed on a 2% agarose gel, and the products were gel-purified using Agarose GelExtract Mini Kit (5Prime) and sequenced.

B-galactosidase activity assay

Exponentially growing anoxic precultures were diluted into fresh oxic medium to an OD₆₀₀ = 0.01 and grown with vigorous shaking for the indicated times. For measurement of *hemH'-lacZ* and *hemH(NI)'-lacZ* expression in strains containing *poxyR2*, overnight cultures grown in oxic LB supplemented with 20 µg ml⁻¹ chloramphenicol were diluted into oxic medium to an OD₆₀₀ = 0.005 and grown until the mid-log phase at an OD₆₀₀ ~ 0.1. Cells were harvested by centrifuging 25 ml at 7000 × g at 4°C for 10 min. Cell pellets were washed in 20 ml cold 0.05 M Tris-Cl (pH 8) and resuspended in 1 ml of the same buffer solution. The cells were lysed by French press, and the cell debris was removed by centrifu-

gation at 12 000 × g at 4°C for 10 min. Supernatants were then assayed for β-galactosidase activity using ONPG as substrate. Accumulation of the reaction product o-nitrophenol was monitored at 420 nm (Miller, 1972). Protein concentrations of the supernatants were measured by Bradford protein assay and were used to normalize the β-galactosidase specific activities.

KatG peroxidase activity assay

The wild-type KatG enzyme functions in vivo as a catalase, but it also possesses a small amount of dye-oxidizing peroxidase activity that is physiologically insignificant but which can be used to quantify the active form of the enzyme in cell extracts. In this study, we frequently employed a mutant form of the enzyme, denoted KatGΔFG, which lacks the catalase activity but retains the peroxidase activity (Li and Goodwin, 2004). In these strains, this activity was used to appraise the efficiency with which heme was being supplied to the KatG enzyme. For peroxidase assays, anoxic precultures in glucose medium were diluted into 100 ml of fresh oxic medium ± 10 µM MnCl₂ to an OD₆₀₀ = 0.02. Cells were grown aerobically with a vigorous shaking for 3 h prior to harvesting. For strains carrying the *poxyR2* plasmid, the media included 20 µg ml⁻¹ chloramphenicol. Cells were washed twice in 20 ml cold 0.05 KPi (pH 7.8), resuspended in 1 ml 0.01 M KPi (pH 6.4) and lysed by sonication. Cell debris was removed by centrifuging at 12 000 × g at 4°C for 10 min, and the supernatants were used to assay the KatG peroxidase activity by the o-dianisidine method (Messner and Imlay, 1999). Briefly, extracts were added to 0.3 mM o-dianisidine and 10 mM KPi (pH 6.4). To start the reaction, 0.9 mM and 9 mM H₂O₂ were added to measure peroxidase activity of extracts containing KatG and KatGΔFG respectively. The oxidation of o-dianisidine was monitored at A₄₆₀. Protein concentrations of the supernatants were measured by Bradford protein assay and were used to normalize the peroxidase-specific activities.

NADH dehydrogenase assay

Anoxic precultures in glucose medium were diluted into 150 ml of fresh oxic medium ± 10 µM MnCl₂ to an OD₆₀₀ = 0.02. Cells were grown aerobically with a vigorous shaking until they reached an OD₆₀₀ = 0.15–0.2. Cells were washed twice with ice-cold 50 mM MES buffer (pH 6) and resuspended in 4 ml of the same buffer solution. Cells were lysed by French press, forming inverted membrane vesicles, and the cell debris was removed by centrifugation for 20 min at 12 000 × g at 4°C. The supernatant, which contained the vesicles, was centrifuged at 100 000 × g at 4°C for 2 h and then resuspended in 1 ml pre-chilled 50 mM MES (pH 6). MES was used as the buffer because the NADH dehydrogenase I complex is unstable at higher pH. NADH (120 µM) was added to the membranes inverted vesicles, and the total NADH oxidase activity was monitored according to the decrease of A₃₄₀. This activity represents electron flow from NADH through the NADH dehydrogenase complexes, the quinone pool, and the terminal cytochrome oxidases. The NADH dehydrogenase activities themselves were assayed by measurement of NADH:ferricyanide oxidoreductase activi-

ity, which depends solely on the dehydrogenases themselves. The inverted vesicles were preincubated with 3 mM KCN to irreversibly inhibit ~95% of cytochrome oxidase activity. Then 200 μ M K₃Fe(CN)₆ was added, and absorbance at 420 nm was monitored (Siegel *et al.*, 1974).

H₂O₂ assays

Bacterial membranes have significant but not unlimited permeability to H₂O₂. Therefore, in hydroperoxidase-deficient (Hpx⁻) cells, which lack significant scavenging activity ($\Delta katG$ $\Delta katE$ $\Delta ahpCF$), H₂O₂ rapidly equilibrates in and out the cells, making the extra- and intracellular H₂O₂ concentrations nearly identical (Seaver and Imlay, 2001b).

For measurements of H₂O₂ accumulation, Hpx⁻ cells were precultured in glucose medium containing aromatic and histidine amino acids. The exponentially growing cells (OD₆₀₀ of ~0.1) were diluted to OD₆₀₀ = 0.005 into 25 ml fresh oxic medium of the same composition and grown with vigorous shaking. At intervals 1 ml of the cultures was removed, cells were removed from this aliquot by filtration, and the filtrates were frozen on dry ice. The H₂O₂ concentrations of the filtrates were measured by the Amplex Red/horseradish peroxidase method as described previously (Seaver and Imlay, 2001a).

In some experiments hydroperoxidase-proficient cells were monitored for the rate at which they degraded a bolus of exogenous H₂O₂. Precultures in anoxic LB medium were diluted to an OD₆₀₀ = 0.005 into 25 ml fresh oxic LB containing the indicated H₂O₂ concentrations, and cultures were incubated with vigorous shaking. At regular intervals, 1 ml of the cultures was removed, the cells were pelleted by centrifugation for 1 min at 12 000 $\times g$ at room temperature, and the supernatants were transferred to fresh Eppendorf tubes and frozen on dry ice. The H₂O₂ concentrations of supernatants were determined as described previously (Wolff, 1994). The method involves the oxidation of ferrous ions by H₂O₂ at low pH via Fenton chemistry, producing ferric ions that form a colored adduct with the xylenol orange dye. Accumulation of this complex was monitored at 560 nm. A standard curve was generated with known amounts of H₂O₂.

H₂O₂ killing assay

Precultures in anoxic LB medium were diluted to an OD₆₀₀ = 0.001 in fresh oxic LB containing 0.5 mM H₂O₂, and cultures were incubated at 37 °C under vigorous shaking. At regular intervals, aliquots of cells were removed and serially diluted in LB before being plated on LB plates. Colonies were enumerated after overnight incubation at 37°C.

Disk diffusion assay

Cells were grown overnight in oxic LB medium to stationary phase. These overnight cultures were diluted in fresh oxic LB to an OD₆₀₀ = 0.005 and incubated to OD₆₀₀ ~ 0.1. Cell numbers were equalized by the final OD₆₀₀ in 100 μ l LB, mixed with 4 ml LB-top agar (0.8%) and spread on LB plates. After 30 min incubation at RT, a 6 mm round paper disk presoaked with 15 μ l 1 M H₂O₂ (10 mM for the $\Delta katG$ strains)

was deposited on the center of the plate. After 24 h incubation at 37°C, the diameter of the zone of growth inhibition around the disk was measured. For the experiments performed with strains carrying pCKR101, pdpr and pdps, the media and plates were supplemented with 100 μ g ml⁻¹ ampicillin and 1 mM IPTG.

Western blot analysis

Anoxic precultures in glucose medium were diluted into 100 ml of fresh oxic medium ± 10 μ M MnCl₂ to an OD₆₀₀ = 0.01, and cells were grown with vigorous shaking in the open laboratory for 3 h. The cells were centrifuged at 7000 $\times g$ at 4°C for 10 min, washed in 20 ml cold 0.05 M Tris-Cl (pH 8), and resuspended in 1 ml of the same buffer solution. Cells were lysed by sonication, and the cell debris was removed by centrifugation at 12 000 $\times g$ at 4°C for 10 min. The protein concentrations of the lysates were measured by Bradford protein assay. Ten micrograms of each protein sample was separated by 12% SDS-PAGE and transferred to nitrocellulose membranes. After blotting with a 5% skim milk solution, 1:100 dilution of rabbit serum containing either anti-HemA or anti-KatG was used as primary antibody. The rabbit serum containing anti-KatG IgG had previously been incubated with 4 mg of protein extract of the Hpx⁻ strain (which lacks KatG) to increase the specificity of the primary antibody. A 1:2000 dilution of horseradish peroxidase-conjugated anti-rabbit goat IgG was used as the secondary antibody, and the bands were detected by chemiluminescence with the ECL Western Blotting Detection Reagents.

Extraction of porphyrins

Anaerobic precultures in glucose medium were diluted into 400 ml of fresh oxic medium ± 10 μ M MnCl₂ to an OD₆₀₀ = 0.02 and grown aerobically under vigorous shaking in the open laboratory for 3 h. Intracellular porphyrins were extracted using a modified procedure (Nakayashiki and Inokuchi, 1997). Cells were centrifuged at 7000 $\times g$ at 4°C for 10 min and washed in 20 ml cold 0.05 M Tris (pH 8)/2 mM EDTA. Cells were resuspended in 10 ml of the same buffer. The OD₆₀₀ was measured to equalize the cell number of each sample. After centrifugation at 7000 $\times g$ at 4°C for 10 min, the cell pellets were resuspended in 1 ml ethyl acetate/glacial acetic acid (3:1, v/v). The cells were lysed by sonication on ice. Cell debris was removed by centrifugation at 7000 $\times g$ at 4°C for 10 min. The nonaqueous layer was washed two times with 1 ml H₂O. Porphyrins were extracted from the organic solvent by the addition of 100 μ l of 3 M HCl. After a vigorous shaking the aqueous solution was transferred to a fresh Eppendorf tube and submitted for LC/MS/MS analysis.

LC/MS/MS analysis

Samples were analyzed by the UIUC Metabolomics Center with the 5500 QTRAP LC/MS/MS system (AB Sciex, Foster City, CA, USA) using a 1200 series HPLC system (Agilent Technologies, Santa Clara, CA, USA) including a degasser, an autosampler and a binary pump. The LC separation was performed on an Agilent SB-Aqcolumn (4.6 × 50 mm, 5 μ m)

(Santa Clara, CA, USA) with mobile phase A (0.1% formic acid in water) and mobile phase B (0.1% formic acid in acetonitrile). The flow rate was 0.3 ml/min. The linear gradient was as follows: 0–1 min, 100% A; 10–18 min, 5% A; 19–24 min, 100% A. The autosampler was set at 5°C. The injection volume was 1 µL. Mass spectra were acquired with positive electrospray ionization, and the ion spray voltage was 5500 V. The source temperature was 450°C. The curtain gas, ion source gas 1 and ion source gas 2 were 32, 65 and 50 respectively. Multiple reactions monitoring were used to monitor coproporphyrin III (m/z 655.4 → m/z 596.3) and protoporphyrin IX (m/z 563.2 → m/z 504.1).

Statistical analysis

Error bars in all figures represent the standard deviations of values drawn from at least three biological replicates.

Acknowledgements

We are very grateful to Douglas Goodwin (Auburn University) for providing the *pkatGΔFG* plasmid, Peter Loewen (University of Manitoba) for donating the anti-KatG antibody, and Li Zhong (Metabolomics Center, University of Illinois) for the LC/MS/MS analysis. This work was supported by grant GM49640 from the National Institutes of Health and by award number PBBEP3_139397 from the Swiss National Science Foundation.

References

- Altuvia, S., Almiron, M., Huisman, G., Kolter, R., and Storz, G. (1994) The *dps* promoter is activated by OxyR during growth and by IHF and sigma S in stationary phase. *Mol Microbiol* **13**: 265–272.
- Andrews, S.C., Robinson, A.K., and Rodriguez-Quinones, F. (2003) Bacterial iron homeostasis. *FEMS Microbiol Rev* **27**: 215–237.
- Anjem, A., and Imlay, J.A. (2012) Mononuclear iron enzymes are primary targets of hydrogen peroxide stress. *J Biol Chem* **287**: 15544–15556.
- Anjem, A., Varghese, S., and Imlay, J.A. (2009) Manganese import is a key element of the OxyR response to hydrogen peroxide in *Escherichia coli*. *Mol Microbiol* **72**: 844–858.
- Asad, L.M.B.O., Asad, N.R., Silva, A.B., Almeida, C.E.B.D., and Leitao, A.C. (1997) Role of SOS and OxyR systems in the repair of *Escherichia coli* submitted to hydrogen peroxide under low iron conditions. *Biochimie* **79**: 359–364.
- Aslund, F., Zheng, M., Beckwith, J., and Storz, G. (1999) Regulation of the OxyR transcription factor by hydrogen peroxide and the cellular thiol-disulfide status. *Proc Natl Acad Sci USA* **96**: 6161–6165.
- Azzouzi, A., Steunou, A.-S., Durand, A., Khalfaoui-Hassani, B., Bourbon, M.-L., Astier, C., et al. (2013) Coproporphyrin III excretion identifies the anaerobic coproporphyrinogen III oxidase HemN as a copper target in the Cu⁺-ATPase mutant *copA*⁻ of *Rubrivivax gelatinosus*. *Mol Microbiol* **88**: 339–351.
- Baureder, M., and Hederstedt, L. (2013) Heme proteins in lactic acid bacteria. *Adv Microb Physiol* **62**: 1–43.
- Bedard, K., Lardy, B., and Krause, K.-H. (2007) NOX family NADPH oxidases: not just in mammals. *Biochemie* **89**: 1107–1112.
- Breckau, D., Mahlitz, E., Sauerwald, A., Layer, G., and Jahn, D. (2003) Oxygen-dependent coproporphyrinogen III oxidase (HemF) from *Escherichia coli* is stimulated by manganese. *J Biol Chem* **278**: 46625–46631.
- Burton, N.A., Schurmann, N., Casse, O., Steeb, A.K., Claudi, B., Zanki, J., et al. (2014) Disparate impact of oxidative host defenses determines the fate of *Salmonella* during systemic infection in mice. *Cell Host & Microbe* **15**: 72–83.
- Cavallaro, G., Decaria, L., and Rosato, A. (2008) Genome-based analysis of heme biosynthesis and uptake in prokaryotic systems. *J Proteome Res* **7**: 4946–4954.
- Chiancone, E., and Ceci, P. (2010) The multifaceted capacity of Dps proteins to combat bacterial stress conditions: detoxification of iron and hydrogen peroxide and DNA binding. *Biochim Biophys Acta* **1800**: 798–805.
- Courcelle, J., Khodursky, A., Peter, B., Brown, P.O., and Hanawalt, P.C. (2001) Comparative gene expression profiles following UV exposure in wild-type and SOS-deficient *Escherichia coli*. *Genetics* **158**: 41–64.
- Datsenko, K.A., and Wanner, B.L. (2000) One-step inactivation of chromosomal genes in *Escherichia coli* K-12 using PCR products. *Proc Natl Acad Sci USA* **97**: 6640–6645.
- Djoko, K.Y., and McEwan, A.G. (2013) Antimicrobial action of copper is amplified via inhibition of heme biosynthesis. *ACS Chem Biol* **8**: 2217–2223.
- Dupont, C.L., Grass, G., and Rensing, C. (2011) Copper toxicity and the origin of bacterial resistance – new insights and applications. *Metallooms* **3**: 1109–1118.
- Dwyer, D.J., Belenky, P.A., Yang, J.H., MacDonald, I.C., Martell, J.D., Takahashi, N., et al. (2014) Antibiotics induce redox-related physiological alterations as part of their lethality. *Proc Natl Acad Sci USA* **111**: E2100–E2109.
- Faulkner, M.J., Ma, Z., Fuangthong, M., and Helmann, J.D. (2012) Derepression of the *Bacillus subtilis* PerR peroxide stress response leads to iron deficiency. *J Bacteriol* **194**: 1226–1235.
- Fridovich, I. (1986) Superoxide dismutases. *Adv Enz* **58**: 61–97.
- Glass, G.A., DeLisle, D.M., DeTogni, P., Gabig, T.G., Magee, B.H., Markert, M., and Babior, B.M. (1986) The respiratory burst oxidase of human neutrophils. Further studies of the purified enzyme. *J Biol Chem* **261**: 13247–13251.
- Goerlich, O., Quillardet, P., and Hofnung, M. (1989) Induction of the SOS response by hydrogen peroxide in various *Escherichia coli* mutants with altered protection against oxidative DNA damage. *J Bact* **171**: 6141–6147.
- Gu, M., and Imlay, J.A. (2011) The SoxRS response of *Escherichia coli* is directly activated by redox-cycling drugs rather than by superoxide. *Mol Microbiol* **79**: 1136–1150.
- Haldimann, A., and Wanner, B.L. (2001) Conditional-replication, integration, excision, and retrieval plasmid-host systems for gene structure-function studies of bacteria. *J Bacteriol* **183**: 6384–6393.
- Hasan, N., Koob, M., and Szybalski, W. (1994) *Escherichia coli* genome targeting, I. Cre-lox-mediated in vitro generation of ori- plasmids and their in vivo chromosomal integration and retrieval. *Gene* **150**: 51–56.
- Helmann, J.D., Wu, M.F.W., Gaballa, A., Kobel, P.A.,

- Morshed, M.M., Fawcett, P., and Paddon, C. (2003) The global transcriptional response of *Bacillus subtilis* to peroxide stress is coordinated by three transcription factors. *J Bacteriol* **185**: 243–253.
- Ilari, A., Ceci, P., Ferrari, D., Rossi, G., and Chiancone, E. (2002) Iron incorporation into *E. coli* Dps gives rise to a ferritin-like microcrystalline core. *J Biol Chem* **277**: 37619–37623.
- Imlay, J.A. (2009) Oxidative stress. In *EcoSal–Escherichia coli and Salmonella: Cellular and Molecular Biology*. Bock, A., Curtiss, R., III Kaper, J.B., Karp, P.D., Neidhardt, F.C., Nystrom, T., et al. (eds). Washington, DC: ASM Press. <http://www.ecosal.org>
- Imlay, J.A. (2013) The molecular mechanisms and physiological consequences of oxidative stress: lessons from a model bacterium. *Nat Rev Microbiol* **11**: 443–454.
- Imlay, J.A., Chin, S.M., and Linn, S. (1988) Toxic DNA damage by hydrogen peroxide through the Fenton reaction in vivo and in vitro. *Science* **240**: 640–642.
- Jacobson, F.S., Morgan, R.W., Christman, M.F., and Ames, B.N. (1989) An alkyl hydroperoxide reductase from *Salmonella typhimurium* involved in the defense of DNA against oxidative damage. Purification and properties. *J Biol Chem* **264**: 1488–1496.
- Jang, S., and Imlay, J.A. (2007) Micromolar intracellular hydrogen peroxide disrupts metabolism by damaging iron-sulfur enzymes. *J Biol Chem* **282**: 929–937.
- Jang, S., and Imlay, J.A. (2010) Hydrogen peroxide inactivates the *Escherichia coli* Isc iron-sulphur assembly system, and OxyR induces the Suf system to compensate. *Mol Microbiol* **78**: 1448–1467.
- Jones, A.M., and Elliott, T. (2010) A purified mutant HemA protein from *Salmonella enterica* serovar *Typhimurium* lacks bound heme and is defective for heme-mediated regulation in vivo. *FEMS Microbiol Lett* **307**: 41–47.
- Jovanovic, G., Mehta, P., McDonald, C., Davidson, A.C., Uzdavins, P., Ying, L., and Buck, M. (2014) The N-terminal amphipathic helices determine regulatory and effector functions of phage shock protein A (PspA) in *Escherichia coli*. *J Mol Biol* **426**: 1498–1511.
- Kehres, D.G., Janakiraman, A., Slauch, J.M., and Maguire, M.E. (2002) Regulation of *Salmonella enterica* serovar *Typhimurium* *mnhH* transcription by H₂O₂, Fe²⁺, and Mn²⁺. *J Bacteriol* **184**: 3151–3158.
- Layer, G., Pierik, A.J., Trost, M., Rigby, S.E., Leech, H.K., Grage, K., et al. (2006) The substrate radical of *Escherichia coli* oxygen-independent coproporphyrinogen III oxidase HemN. *J Biol Chem* **281**: 15727–15734.
- Lee, C., Lee, S.M., Mukhopadhyay, P., Kim, S.J., Lee, S.C., Ahn, W.S., et al. (2004) Redox regulation of OxyR requires specific disulfide bond formation involving a rapid kinetic reaction path. *Nat Struct Mol Biol* **11**: 1179–1185.
- Lee, J., Hiibel, S.R., Reardon, K.F., and Wood, T.K. (2009) Identification of stress-related proteins in *Escherichia coli* using the pollutant *cis*-dichloroethylene. *J Appl Microbiol* **108**: 2088–2102.
- Lee, J.W., and Helmann, J.D. (2006) The PerR transcription factor senses H₂O₂ by metal-catalyzed histidine oxidation. *Nature* **440**: 363–367.
- Li, G.-W., Burkhardt, D., Gross, C., and Weissman, J.S. (2014) Quantifying absolute protein synthesis rates reveals principles underlying allocation of cellular resources. *Cell* **157**: 624–635.
- Li, Y., and Goodwin, D.C. (2004) Vital roles of an interhelical insertion in catalase-peroxidase bifunctionality. *Biochem Biophys Res Commun* **318**: 970–976.
- Manchado, M., Michan, C., and Pueyo, C. (2000) Hydrogen peroxide activates the SoxRS regulon in vivo. *J Bacteriol* **182**: 6842–6844.
- Massey, V., Strickland, S., Mayhew, S.G., Howell, L.G., Engel, P.C., Matthews, R.G., et al. (1969) The production of superoxide anion radicals in the reaction of reduced flavins and flavoproteins with molecular oxygen. *Biochem Biophys Res Commun* **36**: 891–897.
- Mehdy, M.C. (1994) Active oxygen species in plant defense against pathogens. *Plant Physiol* **105**: 467–472.
- Messner, K.R., and Imlay, J.A. (1999) The identification of primary sites of superoxide and hydrogen peroxide formation in the aerobic respiratory chain and sulfite reductase complex of *Escherichia coli*. *J Biol Chem* **274**: 10119–10128.
- Miller, J.H. (1972) *Experiments in Molecular Genetics*. Cold Spring Harbor Laboratory, Cold Spring Harbor, N.Y.
- Miyamoto, K., Nakahigashi, K., Nishimura, K., and Inokuchi, H. (1991) Isolation and characterization of visible light-sensitive mutants of *Escherichia coli* K12. *J Mol Biol* **219**: 393–398.
- Mobius, K., Arias-Cartin, R., Breckau, D., Hannig, A.-L., Riedmann, K., Biedendieck, R., et al. (2010) Heme biosynthesis is coupled to electron transport chains for energy generation. *Proc Natl Acad Sci USA* **107**: 10436–10441.
- Morgan, R.W., Christman, M.F., Jacobson, F.S., Storz, G., and Ames, B.N. (1986) Hydrogen peroxide-inducible proteins in *Salmonella typhimurium* overlap with heat-shock and other stress proteins. *Proc Natl Acad Sci USA* **83**: 8059–8063.
- Mukhopadyay, S., and Schellhorn, H.E. (1997) Identification and characterization of hydrogen peroxide-sensitive mutants of *Escherichia coli*: genes that require OxyR for expression. *J Bacteriol* **179**: 330–338.
- Nachin, L., Loiseau, L., Expert, D., and Barras, F. (2003) SufC: an unorthodox cytoplasmic ABC ATPase required for [Fe-S] biogenesis under oxidative stress. *EMBO J* **22**: 427–437.
- Nakayashiki, T., and Inokuchi, H. (1997) Effects of starvation for heme on the synthesis of porphyrins in *Escherichia coli*. *Mol Gen Genet* **255**: 376–381.
- Outten, F.W., Djaman, O., and Storz, G. (2004) A suf operon requirement for Fe-S cluster assembly during iron starvation in *Escherichia coli*. *Mol Microbiol* **52**: 861–872.
- Park, S., You, X., and Imlay, J.A. (2005) Substantial DNA damage from submicromolar intracellular hydrogen peroxide detected in Hpx[−] mutants of *Escherichia coli*. *Proc Natl Acad Sci USA* **102**: 9317–9322.
- Parsonage, D., Karplus, P.A., and Poole, L.B. (2008) Substrate specificity and redox potential of AhpC, a bacterial peroxiredoxin. *Proc Natl Acad Sci USA* **105**: 8209–8214.
- Pericone, C.D., Park, S., Imlay, J.A., and Weiser, J.N. (2003) Factors contributing to hydrogen peroxide resistance in *Streptococcus pneumoniae* include pyruvate oxidase (SpxB) and avoidance of the toxic effects of the Fenton reaction. *J Bacteriol* **185**: 6815–6825.

- Py, B., and Barras, F. (2010) Building Fe-S proteins: bacterial strategies. *Nat Rev Microbiol* **8**: 436–446.
- Rai, P., Cole, T.D., Wemmer, D.E., and Linn, S. (2001) Localization of Fe²⁺ at an RTGR sequence within a DNA duplex explains preferential cleavage by Fe²⁺ and H₂O₂. *J Mol Biol* **312**: 1089–1101.
- Roche, B., Aussel, L., Ezraty, B., Mandin, P., Py, B., and Barras, F. (2013) Iron/sulfur proteins biogenesis in prokaryotes: formation, regulation and diversity. *Biochim Biophys Acta* **1827**: 455–469.
- Rompf, A., Hungerer, C., Hoffmann, T., Lindenmeyer, M., Romling, U., Gross, U., et al. (1998) Regulation of *Pseudomonas aeruginosa* hemF and hemN by the dual action of the redox response regulators Anr and Dnr. *Mol Microbiol* **29**: 985–997.
- Rush, J.D., Maskos, Z., and Koppenol, W.H. (1990) Distinction between hydroxyl radical and ferryl species. *Meth Enzymol* **186**: 148–156.
- Schook, P.O., Stohl, E.A., Criss, A.K., and Seifert, H.S. (2011) The DNA-binding activity of the *Neisseria gonorrhoeae* LexA orthologue NG1427 is modulated by oxidation. *Mol Microbiol* **79**: 846–860.
- Seaver, L.C., and Imlay, J.A. (2001a) Alkyl hydroperoxide reductase is the primary scavenger of endogenous hydrogen peroxide in *Escherichia coli*. *J Bacteriol* **183**: 7173–7181.
- Seaver, L.C., and Imlay, J.A. (2001b) Hydrogen peroxide fluxes and compartmentalization inside growing *Escherichia coli*. *J Bacteriol* **183**: 7182–7189.
- Severance, S., and Hamza, I. (2009) Trafficking of heme and porphyrins in metazoa. *Chem Rev* **109**: 4596–4616.
- Siegel, L.M., Davis, P.S., and Kamin, H. (1974) Reduced nicotinamide adenine dinucleotide phosphate-sulfite reductase of enterobacteria. III. The *Escherichia coli* hemo-flavoprotein: catalytic parameters and the sequence of electron flow. *J Biol Chem* **249**: 1572–1586.
- Sobota, J.M., and Imlay, J.A. (2011) Iron enzyme ribulose-5-phosphate 3-epimerase in *Escherichia coli* is rapidly damaged by hydrogen peroxide but can be protected by manganese. *Proc Natl Acad Sci USA* **108**: 5402–5407.
- Sobota, J.M., Gu, M., and Imlay, J.A. (2014) Intracellular hydrogen peroxide and superoxide poison 3-deoxy-D-arabinoheptulosonate 7-phosphate synthase, the first committed enzyme in the aromatic biosynthetic pathway of *Escherichia coli*. *J Bacteriol* **196**: 1980–1991.
- Srinivasan, C., Liba, A., Imlay, J.A., Valentine, J.S., and Gralla, E.B. (2000) Yeast lacking superoxide dismutase(s) show elevated levels of ‘free iron’ as measured by whole cell electron paramagnetic resonance. *J Biol Chem* **275**: 29187–29192.
- Stephani, K., Weichert, D., and Hengge, R. (2003) Dynamic control of Dps protein levels by ClpXP and ClpAP proteases in *Escherichia coli*. *Mol Microbiol* **49**: 1605–1614.
- Touati, D., Jacques, M., Tardat, B., Bouchard, L., and Despied, S. (1995) Lethal oxidative damage and mutagenesis are generated by iron in delta fur mutants of *Escherichia coli*: protective role of superoxide dismutase. *J Bacteriol* **177**: 2305–2314.
- Troup, B., Hungerer, C., and Jahn, D. (1995) Cloning and characterization of the *Escherichia coli* hemN gene encoding the oxygen-independent coproporphyrinogen III oxidase. *J Bacteriol* **177**: 3326–3331.
- Tucker, N.P., D'Autreux, B., Yousafzai, F.K., Fairhurst, S.A., Spiro, S., and Dixon, R. (2008) Analysis of the nitric oxide-sensing non-heme iron center in the NorR regulatory protein. *J Biol Chem* **283**: 908–918.
- Varghese, S., Wu, A., Park, S., Imlay, K.R.C., and Imlay, J.A. (2007) Submicromolar hydrogen peroxide disrupts the ability of Fur protein to control free-iron levels in *Escherichia coli*. *Mol Microbiol* **64**: 822–830.
- Wang, L., Elliott, M., and Elliott, T. (1999) Conditional stability of the HemA protein (glutamyl-tRNA reductase) regulates heme biosynthesis in *Salmonella typhimurium*. *J Bacteriol* **181**: 1211–1219.
- Wang, L.Y., Brown, L., Elliott, M., and Elliott, T. (1997) Regulation of heme biosynthesis in *Salmonella typhimurium*: activity of glutamyl-tRNA reductase (HemA) is greatly elevated during heme limitation by a mechanism which increases abundance of the protein. *J Bacteriol* **179**: 2907–2914.
- Wenk, M., Ba, Q., Erichsen, V., MacInnes, K., Wiese, H., Warscheid, B., and Koch, H.G. (2012) A universally conserved ATPase regulates the oxidative stress response in *Escherichia coli*. *J Biol Chem* **287**: 43585–43598.
- Winterbourn, C.C., Hampton, M.B., Livesey, J.H., and Kettle, A.J. (2006) Modeling the reactions of superoxide and myeloperoxidase in the neutrophil phagosome. Implications for microbial killing. *J Biol Chem* **281**: 39860–39869.
- Wolff, S.P. (1994) Ferrous ion oxidation in presence of ferric ion indicator xylenol orange for measurement of hydroperoxides. *Meth Enzymol* **233**: 182–189.
- Woodard, S.I., and Dailey, H.A. (1995) Regulation of heme biosynthesis in *Escherichia coli*. *Arch Biochem Biophys* **316**: 110–115.
- Yamamoto, K., Ishihama, A., Busby, S.J., and Grainger, D.C. (2011) The *Escherichia coli* K-12 MntR miniregulon includes dps, which encodes the major stationary-phase DNA-binding protein. *J Bacteriol* **193**: 1477–1480.
- Zheng, M., Wang, X., Templeton, L.J., Smulski, D.R., LaRossa, R.A., and Storz, G. (2001) DNA microarray-mediated transcriptional profiling of the *Escherichia coli* response to hydrogen peroxide. *J Bacteriol* **183**: 4562–4570.

Supporting information

Additional supporting information may be found in the online version of this article at the publisher's web-site.